University of Calgary

PRISM Repository **https://prism.ucalgary.ca**

The Vault Open Theses and Dissertations

2017

Modelling of the Thermodynamic Equilibrium Conditions for the Formation of TBAB Semi-Clathrates Formed by gas mixtures of Carbon Dioxide, Nitrogen, Hydrogen, Methane and Carbon Monoxide

Cyprian Jerard, Naveen Michel Raj

Cyprian Jerard, N. M. (2017). Modelling of the Thermodynamic Equilibrium Conditions for the Formation of TBAB Semi-Clathrates Formed by gas mixtures of Carbon Dioxide, Nitrogen, Hydrogen, Methane and Carbon Monoxide (Master's thesis, University of Calgary, Calgary, Canada). Retrieved from https://prism.ucalgary.ca. doi:10.11575/PRISM/26959

http://hdl.handle.net/11023/3621

Downloaded from PRISM Repository, University of Calgary

UNIVERSITY OF CALGARY

Modelling of the Thermodynamic Equilibrium Conditions for the Formation of TBAB Semi-Clathrates Formed by gas mixtures of Carbon Dioxide, Nitrogen, Hydrogen, Methane and Carbon Monoxide

Naveen Michel Raj Cyprian Jerard

by

A THESIS

SUBMITTED TO THE FACULTY OF GRADUATE STUDIES

IN PARTIAL FULFILMENT OF THE REQUIREMENTS FOR THE

DEGREE OF MASTERS OF ENGINEERING

GRADUATE PROGRAM IN CHEMICAL ENGINEERING

CALGARY, ALBERTA

JANUARY 2017

© Naveen Michel Raj Cyprian Jerard 2017

Abstract

Semi-clathrates are ice like crystalline substance which are like that of gas hydrates. Like clathrate hydrates, the semi-clathrates can entrap gas molecules in its molecular framework. Since semi-clathrate are formed at much milder conditions when compared with the clathrate hydrate. Thus, in the recent years, there has been much interest in using semi-clathrate in applications such as gas storage and separation. The aim of the present study is to measure the dissociation condition of semi-clathrate formed from Tetra-*n*-butyl ammonium bromide in the presence of the gas mixtures using a developed thermodynamic model.

The developed thermodynamic model the PSRK equation of state is used to describe the vapour phase, the LIFAC activity coefficient model is used to compute the activity coefficient in the liquid phase. The van der Waals and Platteeuw theory is employed to describe the semi-clathrate phase. In this model, the Langmuir constants are calculated using the Kihara potential, whereas most of the previously developed model uses the empirical correlation. The thermodynamic model is used in the present work to predict the dissociation condition of the semi-clathrate formed from Tetra-*n*-butyl ammonium bromide in the presence of the gas mixtures like carbon dioxide (CO_2), carbon monoxide (CO), nitrogen (N_2) and hydrogen (H_2). A good agreement between the experimental and predicted values were observed using this model. The % ARD (average relative deviation) of the calculated and experimental values were in the range of 3.2% to 7.2%.

Acknowledgements

I would first like to thank the God Almighty.

I would like to express my deepest gratitude to my mentor and supervisor Dr. Matthew A. Clarke who provided the opportunity for me to work on this project and, I also wish to thank my supervisor for his patience, continuous support, mentorship, encouragement and supervision of this thesis.

I am thankful to the members of the examining committee for their valuable comments and feedbacks.

I would also like to acknowledge Marlon Garcia for the useful discussions and for his valuable advice.

Finally, I would like to thank my parents for their unconditional love and encouragement throughout the course of this degree.

Table of Contents

List of Tables

List of Figures and Illustrations

List of Symbols, Abbreviations and Nomenclature

Abbreviations	Definition
A	Anion
Br^-	Anion Bromide
C	Cation
C_2H_6	Ethane
C_3H_8	Propane
CA	Salt molecule/ Cation-Anion
CCS	Carbon capture and storage
CH_4	Methane
Cl^-	Anion Chloride
CO_2	Carbon dioxide
DTAC	Dodecyl trimethyl ammonium chloride
DTAC	dodecyl trimethyl ammonium chloride
e-NRTL	Activity coefficient model
EoS	Equation of state
F^-	Anion Fluoride
GHG	Greenhouse gases
H_2	Hydrogen
H_2O	Water
H_2S	Hydrogen sulfide
LIFAC	Activity coefficient model
LNG	Liquefied natural gas

MEA	Monoethanol amine
MW	Molecular weight [$g \cdot mol^{-1}$]
N_2	Nitrogen
O_2	Oxygen
PRO II	Commercial chemical process simulator
PSRK	Predictive-Soave-Redlich-Kwong Equation of state
QAS	Quaternary ammonium salts
SAFT-VRE	Statistical associating fluid theory with variable range for electrolytes
SDC	Sodium dodecyl sulfate
SLE	Solid-liquid equilibria
S-L-V	Solid-liquid-vapour
SRK	Soave-Redlich-Kwong Equation of State
TBAB	Tetra-*n*-butyl ammonium bromide
TBAC	Tetra-*n*-butyl ammonium chloride
$TBANO_3$	Tetra-*n*-butyl ammonium nitrate
TBAOH	Tetra-*n*-butyl ammonium bromide
TBAX	Tetra-*n*-butyl ammonium salts.X=Br^-,Cl^-,F^-
TBPB	Tetra-*n*-butyl phosphonium bromide
THF	Tetrahydrofuran
UNIFAC	Activity coefficient
vdWP	van der Waals and Platteuw
VLE	Vapour-liquid equilibrium
y_{xenon}	Molar fraction of xenon

y_{argon}	Molar fraction of argon

Symbols	**Definitions**
w_{TBAB}	TBAB weight fraction [-]
w_{TBAC}	TBAC weight fraction [-]
Å	angstrom [10^{-10} m]
sI	Structure *I* in hydrates
sII	Structure *II* in hydrates
sH	Structure *H* in hydrates
$n_i^{m_i}$	Nomenclature for polyhedral
n_i	Number of edges in a face type *i*
m_i	Number of faces with n_i edges
5^{12}	Pentagonal dodecahedron
$5^{12}6^2$	Tetrakaidecahedron
$5^{12}6^4$	Hexakaidecahedron
$4^3 5^6 6^3$	Irregular dodecahedron
$5^{12}6^8$	Icosahedron
$5^{12}6^3$	Pentakaidecahedron
MW	Molecular weight [g·mol^{-1}]
pT	Pressure vs. Temperature
w	Weight fraction [-]
ΔH_{dis}	Enthalpy of dissociation [kJ·mol^{-1}·K^{-1}]
K(T)	Standard constant [-]
z_c^+	Charge of the cation [-]

z_a^-	Charge of the anion [-]
ν_w	Number of water molecules[-]
a_h^H	Activity of the hydrate in the solid phase[-]
a_w^L	Activity of water in the liquid phase[-]
a_c^L	Activity of the cation in the liquid phase[-]
a_a^L	Activity of anion in the liquid phase[-]
γ_w^L	Activity coefficients in the liquid phase of water[-]
γ_c^L	Activity coefficients in the liquid phase of cation[-]
γ_a^L	Activity coefficients in the liquid phase of anion[-]
$\mu_h^{0,H}$	Standard chemical potential of the semiclathrate in the hydrate phase [J·mol^{-1}]
$\mu_w^{0,L}$	Standard chemical potential of water in the liquid phase [J·mol^{-1}]
$\mu_c^{0,L}$	Standard chemical potential of cation in the liquid phase [J·mol^{-1}]
$\mu_a^{0,L}$	Standard chemical potential of anion in the liquid phase [J·mol^{-1}]
$\Delta_{dis}G^0(T)$	Standard Gibbs energy of dissociation [J·mol^{-1}]
V_w^L	Molar volume of pure liquid water and semiclathrate [m^3·mol^{-1}]
V_h^H	Molar volume of semiclathrate in solid phase [m^3·mol^{-1}]
$V_c^{\infty,L}$	Partial molar volume of the cation at infinite dilution of the salt [m^3/mol]
$V_a^{\infty,L}$	Partial molar volume of the anion at infinite dilution of the salt [m^3/mol]
x_w	Molar fraction of water in liquid phase[-]
x_c	Molar fraction of cation in liquid phase[-]
x_a	Molar fraction of anion in liquid phase[-]

$C_{p,i}^{L}$	Isobaric heat capacity of compound *i* in the liquid phase [J·mol^{-1} K^{-1}]
$\Delta_{dis}V^{0}(T)$	Change in volume accompanying the dissociation reaction of the semiclathrate [m^{3}·mol^{-1}]
$\Delta_{dis}H^{0}(T)$	Change in enthalpy accompanying the dissociation reaction of the semiclathrate [J·mol^{-1}]
$\Delta_{dis}C_{p}^{0}(T)$	change in heat capacity accompanying the dissociation reaction of the semiclathrate [J·mol^{-1} K^{-1}]
T_{cgr}	Temperature of congruent point [K]
$\mu_{h}^{H,\beta}$	Chemical potential per salt molecule in the empty metastable phase β [J·mol^{-1}]
Y_{ij}	Occupancy fraction of cavities type *i* by the gas molecule of type *j*
C_{ij}	Langmuir constant of the gas molecule of type *j* and cavities type *i* [MPa^{-1}]
k	Boltzmann's constant [1.38 10^{-23} J·K^{-1}]
R_{cell}	Radius of the cavity [10^{-10} m]
a_{i}	Radius of spherical core of component *i* [10^{-10} m]
r	Distance of the guest molecule from the center of the cavity [10^{-10} m]
$w(r)$	Potential energy function for the interaction between the guest molecule and the molecules constituting the cavity [J·mol^{-1}]
a	Radius of spherical molecular core [10^{-10} m]
σ	Collision diameter [10^{-10} m]
ε	Minimum energy [J]
P	Pressure [MPa]

T	Temperature [K]
A_1	PSRK constant [-]
$T_{c,i}$	Critical temperature of *i* compound [K]
$P_{c,i}$,	Critical pressure of *i* compound [MPa]
ω_i	Acentric factor of *i* compound [-]
c_1, c_2, and c_3	Adjustable parameters regressed from vapour pressure experimental data in PSRK [-]
$a_{m,k}$, $b_{m,k}$, and $c_{m,k}$	Interaction parameters in UNIFAC [-]
F	Objective function
NP	Number of points
x_{gas}^{calc}	Calculated molar fraction of the gas in liquid phase
x_{gas}^{exp}	Experimental molar fractions of the gas in liquid phase
γ_i	Activity coefficient of compound *i* in the mixture [-]
γ_i^{LR}	Long range activity coefficient of compound *i* in the mixture[-]
γ_i^{MR}	Middle range activity coefficient of compound *i* in the mixture[-]
γ_i^{SR}	Short range activity coefficient of compound *i* in the mixture[-]
T^{calc}	Calculated dissociation temperatures of the mixture [K]
T^{exp}	Experimental dissociation temperatures of the mixture [K]

Chapter one: **Introduction**

This chapter presents the fundamental background and relevant literature review about the formation of both semi-clathrates and clathrate hydrates. An illustration of different types of structures formed by the clathrates is also presented in this chapter. Different potential industrial applications, such as using semi-clathrates and clathrate hydrates in the separation process of various gases and using it as a source of energy is also presented in this chapter. Finally, a review of the different thermodynamic models and methodologies for computing the three-phase equilibrium conditions is briefly discussed in the final sections of this chapter.

1.1 Clathrate hydrates

This section begins with discussing the fundamental properties of gas hydrates and then explaining the difference between the clathrate hydrates and semi-clathrates, which are the present focus of our study.

In chemistry, clathrate hydrate structures are generally formed by trapping of a molecule of a compound in a structure of another compound (*1*). Specifically, clathrate hydrates are defined as a solid crystalline structure, which consist of water molecules and other small guest molecules. The small guest molecules, which are referred to as the “former”, are enclathrated (trapped) in the cavities formed by solid matrix of water (*1*).

The first researcher to investigate the hydrate compounds was Sir Humphry Davy (*2*), when he noticed an ice like solid that was formed from the mixture of water and chlorine gas at a temperature higher than the freezing point of water (*2*). Later the composition of the chlorine hydrate was reported by Michael Faraday with further experiments (*3*). The stability of the hydrate structure is due to the interaction of the guest molecules and the water lattice by van der Waals forces (*4*). The guest molecule is free to rotate inside the cage, since there is no chemical bonding between the host and the guest molecules (*1*). These are factors that influence the formation of Clathrate hydrates (*1*).

1. The presence of water
2. Elevated pressure
3. Low temperature (typically < 283 K)

4. Small guest molecules (< 9 Å diameter)

1.2 Hydrate structures

Classification of hydrate structures are based on the arrangement of the water molecules in crystal structures. Hydrates exist in one of three crystal structures; structure *I* (sI), structure *II* (sII), and structure *H* (sH). The first two structures are commonly observed in nature whereas the third hydrate structure is mostly observed in laboratory settings. Furthermore, for structure *H* (sH) to be formed it requires a small gelper molecule like methane as well as a hydrate former like cyclopentane (*5*). Table 1.1 summarises the different types of clathrate structure and their characteristics.

Table 1.1: Three types of clathrate hydrate structure and their characteristics (Reproduced from Carroll (*1*))

Structure	I	II	H
Water molecules per unit cell	46	136	34
Cages per unit cell			
Small	6	16	3
Medium	-	-	2
Large	2	8	1
Theoretical formula			
All cages filled	X*.5 3/4 H_2O	X.5 2/3 H_2O	5X. Y**. 34 H_2O
Mole fraction of hydrate former	0.1481	0.15	0.15
Only large cages filled	X.7 2/3 H_2O	X. 17 H_2O	-
Mole fraction of hydrate former	0.1154	0.0556	-
Cavity diameter (Å)			
Small	7.9	7.8	7.8
Medium	-	-	8.1
Large	8.6	9.5	11.2
Volume of unit cell (m^3)	1.728×10^{-27}	5.178×10^{-27}	
Typical formers	CH_4, C_2H_6, H_2S, CO_2	N_2, C_3H_8, iC_4H_{10}	2-methylbutane, 2,2-dimethylbutane, etc.

* Hydrate former
** Structure H former

1.2.1 Structure I

Structure *I* is considered as the simplest hydrate structure (*5*). It consists of 46 water molecules arranged in two dodecahedron cages and two tetrakaidecahedron cages. Dodecahedra are twelve sided polyhedrons with a pentagon on each face and it is denoted as 5^{12}; 12 stands for number of faces and 5 stands for number of edges. Tetrakaidecahedorn cages are fourteen-sided polyhedron with two hexagonal and five pentagonal faces they are denoted as $5^{12}6^2$. Since dodecahedron cages are smaller than the tetrakaidecahedron cages (*1*) the decahedron cages are referred as small cages and the tetrakaidecahedron is referred as large cages. Compounds such as methane, ethane, carbon dioxide and hydrogen sulfide form structure *I* hydrates (*5*).

1.2.2 Structure II

Structure *II* hydrates consist of two kinds of cages. A dodecahedron cage with a twelve sided polyhedron with a pentagon on each face and it is denoted as 5^{12}, and a hexakaidecahedron cage which is a sixteen sided polyhedron with a twelve pentagonal and four hexagonal faces. Structure *II* hydrates consist of 146 water molecules. The compounds that can form structure *II* hydrates are nitrogen, propane and isobutene. The nitrogen occupies both the small and large cages; however, isobutene and propane only occupy the larger cages.

1.2.3 Structure H

Structure *H* hydrates consist of three types of cavities. Three small regular dodecahedra with a twelve sided polyhedron denoted as 5^{12}, two medium size irregular dodecahedra (**t**hey are not spherical) which has six pentagonal faces with three hexagonal faces denoted as $4^3 5^6 6^3$ and one large size irregular icosahedron (a twenty sided polyhedron which is represented as $5^{12}6^8$).

The unit cell of the Structure *H* consists of 34 water molecules. Generally, the small and medium cavities are occupied by the small helper molecules. The large cavities are occupied by the large guest molecules. Examples of Structure *H* hydrate formers include cycloheptane, 2-methylbutane and 2, 2-dimethylbutane (*5*). Figure 1.1 shows the different types of cavities and Figure 1.2 shows the different types of hydrate structure formed structures that can be formed.

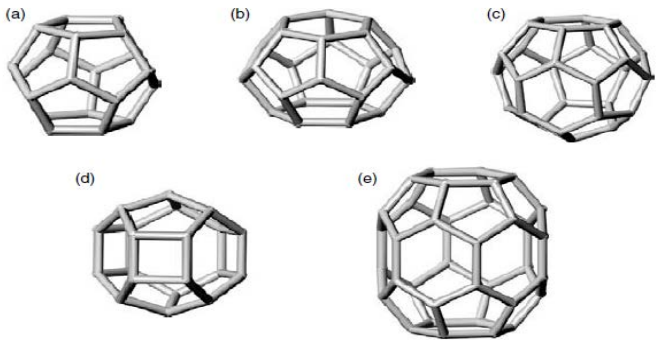

Figure 1.1: Types of cavities (a) pentagonal dodecahedron (5^{12}), (b) Tetrakaidecahedron ($5^{12}6^2$), (c) hexakaidecahedron ($5^{12}6^4$), (d) irregular dodecahedron ($4^35^66^3$), and (e) icosahedron ($5^{12}6^8$) (Reproduced from Sloan and Koh (*5*))

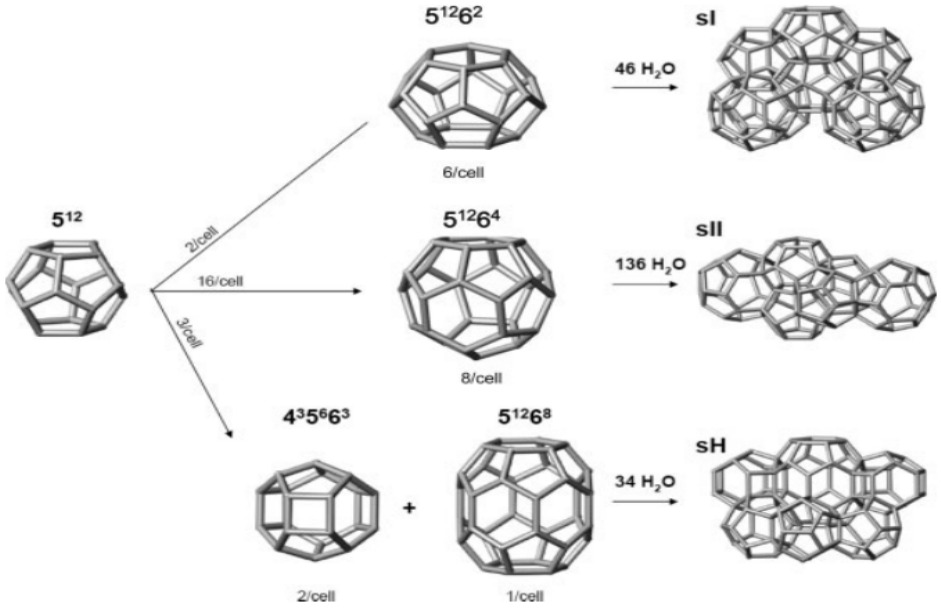

Figure 1.2: Different gas hydrate structures (sI, sII, sH). (Reproduced from Koh and Sloan (*5*))

1.3 Natural gas hydrates

Formation of clathrate hydrates from natural gas constituents can be witnessed in the oil and gas industry. Natural gas, which is a mixture of hydrocarbons (methane, ethane, etc.) and non-hydrocarbons (CO_2, N_2, H_2S, etc.…) is often produced with water as a by-product (*6*). Gas hydrates formed from natural gas can cause the plugging of pipelines in the oil and gas industry. These gas hydrates were first identified in the oil and gas industry in 1934 by Hammerschmidt, who

discovered that it was the clathrate hydrates that were responsible for the plugging of pipelines and not ice (*7*). Even nowadays the gas hydrates still pose a threat to the petroleum industry by causing a risk of blockages in the oil and gas pipelines (*8*). Once a plug is formed in the pipeline it can block the flow of fluids for days or even sometimes weeks (*9*). So, it is in the best interest of the petroleum industries that they prevent the formation of these clathrate hydrates in their pipelines. If a blockage is formed in the pipeline due to the formation of gas hydrates four methodologies are available to remedy the situation: Thermal heating of the pipelines, Depressurization of the pipeline, injecting a hydrate inhibitor at the plug and mechanical removal using coiled tubing (*9*).

1.4 Clathrate Hydrate Promoters

In natural gas transmission, research has been aimed at suppressing the formation of gas hydrates, either by altering the conditions at which they form (i.e. thermodynamic inhibition) or by altering the rate at which they form/agglomerate (i.e. kinetic inhibition). However, in many proposed industrial applications, such as gas storage, it is desirable to promote the formation of gas hydrates. Clathrate hydrate promoters are used as additives to alter the formation condition of the gas hydrate. In other words, using a hydrate promoter, the hydrate can be formed rapidly or at a moderate condition that is at a higher temperature and lower pressure. Some examples of hydrate promoters are tetrahydrofuran (THF) and cyclopentane (*26*). The hydrate promoters are of two types. The first type of promoters does not influence the hydrate crystal structure and are usually encaged in the larger cavities of the hydrate structure, example cyclohexane and tetrahydrofuran (*27*).

The second type of promoters are those that alter the thermodynamic conditions for gas hydrates, usually by changing the crystal structure of the hydrate. Examples of these kinds of promotors include quaternary ammonium salts such as TBAC (tetra-n-butyl ammonium chloride), TBAB (tetra-n-butyl ammonium bromide) and TBAF (tetra-n-butyl ammonium fluoride) (*6*). Since the crystal structure of the hydrate is changed when using the promoters like TBAB and TBAC, these hydrate structure are called as semi-clathrates and they are discussed in detail in the session below.

1.5 Semi-clathrate hydrates

Semi-clathrates have a crystalline structure like that of clathrate hydrates. However, unlike gas hydrates, semi-clathrates also incorporate the anion and cation of the salt into their molecular framework of water molecules. This allows semi-clathrates to form at much milder conditions than gas hydrates. Semi-clathrates can also form without the presence of a guest molecule (*1*). The semi-clathrate was first reported in the literature by Fowler et al (*10*) in the year 1940. Fowler witnessed that when some amount of quaternary ammonium salt, such as Terra-n-Butyl Ammonium Fluoride (TBAF) was added to water, it could form a crystalline structure at room temperature. The dimension of the unit cell, the crystal structure and the hydration numbers were reported by McMullan and Jeffery (*11*) via x-ray diffraction measurements. In 1969 after studying the structure of these crystals through an x-ray and a crystallographic analysis, Jeffery (*12*) decided to term them as semi-clathrates. They were called semi-clathrates because a part of their crystal structure is broken to enclose the Tetra-*n*-Butyl Ammonium cation while the halogen anion such as (Br^-,Cl^-, Fl^-) construct the framework along with water molecules through hydrogen bonding (*13*, *14*). For example, in the case of TBAB, the cation TBA^+ is enclosed in the crystal structure and the anion Br^- incorporates into the framework of water molecules. In the case of the clathrate hydrates the guest molecule is not physically attached to the lattice, it is held by van der Waals forces (*15*). One of the interesting characteristics about semi-clathrates is that they can form crystals by themselves. In other words, unlike clathrate hydrates, semi-clathrates do not require the stabilization effect of the guest molecules to form a crystal (*16*). Figure 1.3 shows a semi-clathrate structure of type B, TBAB.

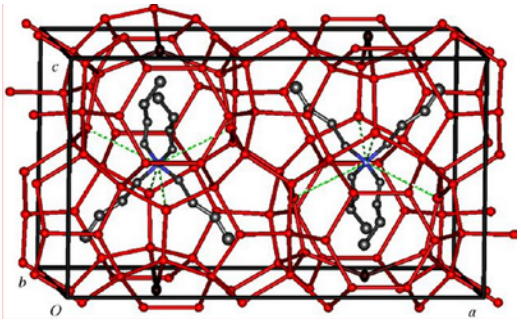

Figure 1.3: Structure of type B, TBAB (Reproduced from Shimada et al (*17*))

1.5.1 Semi-clathrate of TBAB and water

Several authors have investigated the solid-liquid phase behaviour, of the system TBAB + H_2O, in the absence of gases. The main aim of these studies was to determine the crystalline structure formed by the system (TBAB + H_2O), to find the number of water molecule per salt molecule (also known as the hydration number) and finally to measure the congruent melting point of the semi-clathrate structure.

Shimada et al. (*17*) reported a single structure (type *B*), which consist of six dodecahedron cages (5^{12}), four tetrakaidecahedron cages ($5^{12}6^2$) and four Pentakaidecahedron cages ($5^{12}6^3$). Gaponenko et al. (*19*) subsequently OBSERVED four different types of structures (TBAB.24H_2O, TBAB.26H_2O, TBAB.32H_2O and, TBAB.36H_2O). A single structure (type *A*) was observed by Nakayama et al. (*20*) where as Oyama et al. (*21*) observed two types of structure (type A and B). The table 1.2 below shows the various structures reported for semi-clathrate of TBAB and water.

Table 1.2: Experimental studies on TBAB for determining hydration number and congruent melting points. (Reproduced from Garcia (*22*))

Authors	Structure name	Hydration number	Congruent melting temperature/°C
Shimada et al (*17*)	Type *B*	38	N/A
Gaponenko et al (*19*)	TBAB·24H_2O	24	12.4
	TBAB·26H_2O	26	12.2
	TBAB·32H_2O	32	11.6
	TBAB·36H_2O	36	9.5
Oyama et al (*21*)	Type *A*	26	12
	Type *B*	38	9.9
Nakayama et al (*20*)	Type *A*	24	12.9

1.6 Potential Applications of Gas Hydrates and Semi-clathrates

Even though the formation of gas hydrates has always been viewed negatively in the oil and gas industry, there are many potential positive applications of clathrate hydrates and semi-clathrates. These applications include transportation and storage of natural gas, separation of gases like carbon dioxide (CO_2), nitrogen (N_2), hydrogen sulfide (H_2S), methane (CH_4) and hydrogen

(H_2) by the process of hydrate formation (*1*). This section discusses the potential applications of clathrate hydrates and sem-iclathrates.

1.7 Storage and Transportation of Natural Gas

The ability of clathrates or sem-iclathrates to concentrate natural gas in the form of hydrates makes them attractive process for potential use in the storage and transportation of gases, including hydrogen or methane. At standard conditions, it is known that a cubic metre of hydrates can store up to 160 m^3 of methane (*23*). Figure 1.4 outlines a conceptual process diagram of transporting the natural gas in the form of gas hydrates.

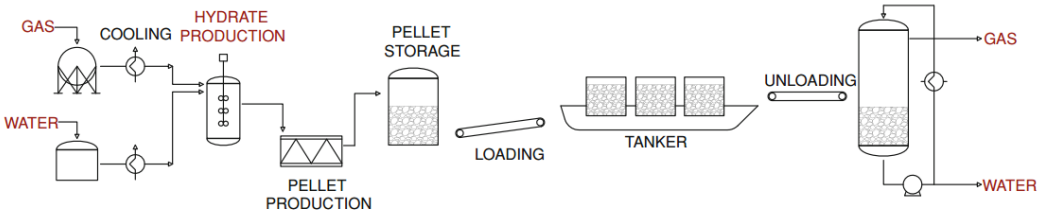

Figure 1.4: Process diagram of transportation of natural gas in the form of gas hydrates. (Reproduced from Garcia (*22*))

One of the main advantages of storing and transportation of natural gas in the form of gas hydrates is safety. For example, when compared with compressed natural gas (CNG) and associated vapours of liquefied natural gas (LNG) the gas in the hydrate form is not explosive, however it is flammable. The transportation of natural gas in the form of gas hydrate is also belived to require less investment in infrastructure and equipment, which considerably lowers the capital cost when compared with other techniques like liquefied natural gas (LNG) (*24*). Hydrogen is one another type of gas molecule that could be stored as a hydrate. The main advantage of hydrogen in a hydrate form is that when a hydrogen hydrate is dissociated the only by-product will be water, which is recyclable.

1.8 Separation process through formation of gas hydrates

The growing energy needs of the world has led to a rapid industrialization, which resulted in high usage of fossil fuel like oil, natural gas and coal (*24*). Due to the combustion of these fossil

fuels, large amounts of greenhouse gases (carbon dioxide, carbon monoxide and hydrogen sulfide) are emitted into the atmosphere (*24*). These greenhouse gases, are believed to be major contributors for the global warming. Since these gases are harmful to the environment, in recent years there is lot of research interest in separating these gases from emissions.

1.8.1 Separation of Carbon dioxide (CO_2)

Carbon dioxide is a greenhouse gas, which is believed to contribute roughly 60% of the greenhouse gas effect in the atmosphere (*24*). Hence, it has become a major concern for the scientific community to capture and/or separate the carbon dioxide from the flue gas streams. Currently, there are many potential techniques being researched for removing CO_2 from pre- and post-combustion streams. In addition to the use of membranes or amine solutions, gas hydrate crystallization is a possible novel method to separate the carbon dioxide from a gas steam. Carbon dioxide can be selectively trapped in clathrate or semi-clathrate phase due to the difference in the affinity of the several hydrate formers to be enclathrated. Once the clathrate or semi-clathrate crystals are formed, the hydrate phase can be enriched with CO_2, while the concentration of other gases in the gas phase can be increased. The carbon dioxide can be recovered from the hydrate phase by dissociating the crystal. Table 1.3 below summarizes some of the experimental studies that have been carried out on separating the carbon dioxide by clathrate/semi-clathrate crystallization in the presence of promoters.

Table 1.3: Experimental studies on semi-clathrate hydrate for carbon dioxide systems in the presence of promoters

Author(s)	Gas System	Aim of study
Sun et al (*28*)	CO_2 + TBAB	Measure the three-phase equilibrium conditions.
Kumar et al (*29*)	CO_2 + TBAB	Kinetic studies.

Author(s)	Gas System	Aim of study
Deschamps et al (*30*)	N_2 + TBAB CO_2 + TBAB N_2 + CO_2 + TBAB CH_4 + CO_2 + TBAB	Measure the three-phase equilibrium conditions.
Wang et al (*31*)	CO_2 + CO + TBAB CO_2 + CO + H_2 + TBAB	Measure the three-phase equilibrium conditions.
Ye et al (*32*)	CO_2 + TBAC CO_2 + TBPC	Measure the three-phase equilibrium conditions.
Mayoufi et al (*33*)	CO_2 + TBPB	Measure the three-phase equilibrium conditions.
Li et al (*34*)	CO_2 + TBAB	Hydrate formation rate.
Lin et al (*35*)	CO_2 + TBAB CO_2 + TBPB	Measure the three-phase equilibrium conditions.
Mohammadi et al (*36*)	CO_2 + TBAB N_2 + TBAB CH_4 + TBAB H_2 + TBAB	Hydrate formation kinetics. Vapour and hydrate phase compositions.
Lin et al (*37*)	CO_2 + TBAB	Measure the three-phase equilibrium conditions.

Author(s)	Gas System	Aim of study
Duc et al (*38*)	$CO_2 + N_2 + TBAB$	Measure the three-phase equilibrium conditions.
Seo et al (*39*)	$CO_2 + THF$	Measure the three-phase equilibrium conditions. and Enthalpies.
Mayoufi et al (*41*)	$CO_2 + TBAB$ $CO_2 + TBAC$ $CO_2 + TBANO_3$ $CO_2 + TBPB$	Measure the three-phase equilibrium conditions. and enthalpies.
Belandria et al (*42*)	$CO_2 + N_2 + TBAB$	Measure the three-phase equilibrium conditions.
Mohammadi et al (*43*)	$CO_2 + N_2 + TBAB$	Measure the three-phase equilibrium conditions.
Li et al (*44*)	$CO_2 + N_2$ + cyclopentane	Hydrate formation kinetics. Vapour and hydrate phase compositions.
Li et al (*45*)	$CO_2 + H_2 + TBAB$	Measure the three-phase equilibrium conditions.
Fan et al (*48*)	$CO_2 + N_2 + TBAB$ $CO_2 + N_2 + TBAF$	Hydrate Formation Rate. Separation efficiency.

Author(s)	Gas System	Aim of study
Li et al (*50*)	$CO_2 + N_2 + TBAB$ $CO_2 + N_2 + DTAC$	Induction time. Separation efficiency.
Meysel et al (*52*)	$CO_2 + N_2 + TBAB$	Measure the three-phase equilibrium conditions. Vapor phase composition.
Kim et al (*53*)	$CO_2 + H_2 + TBAB$	Measure the three-phase equilibrium conditions. Hydrate formation kinetics.

Summary from the literature review of Table 1.3:

Sun et al. (*28*) measured the three-phase equilibrium conditions (solid-liquid-vapour) of semi-clathrates of CO_2 formed in the presence of TBAC, at a temperature range of (282.15 to 291.75) K. The author reported that the addition of TBAC reduced the formation pressure of the semi-clathrate by 2.5 MPa and the stability of the hydrate increased with the increase in the TBAC concentration.

Kumar et al. (*29*) conducted experiments on the CO_2 gas hydrate and studied the effect of the three different silica gels of varying particle size and by using three different surfactants that are non-ionic, cationic and anionic on the hydrate formation. The author concluded that among the three surfactants used, the anionic and non-ionic are more effective when compared with the cationic surfactant. The author also observed that the rate of gas uptake is considerably enhanced in the presence of the silica gel.

Deschamps et al. (*30*) conducted experiments to measure the dissociation conditions of the TBAB semi-clathrates formed from pure gases like N_2, CO_2, CH_4 and gas mixtures ($CO_2 + CH_4$ & $N_2 + CO_2$). The authors determined the dissociation temperature of N_2 and CO_2 semi-clathrate as

a function of TBAB concentration for different pressure of the gas. The concentration of TBAB ranged from 0.170 to 0.400 wt.%.

Wang et al. (*31*) conducted an experiment to measure the three-phase equilibrium condition of TBAB semi-clathrates formed from mixtures of CO_2, CO and H_2. The authors carried out experiments to determine the incipient equilibrium condition for the semi-clathrate of TBAB that were formed from two binary mixtures (CO_2 + H_2 & CO_2 + CO) and from a ternary gas mixture (CO_2 + H_2 + CO). This was the first study that has been carried out for TBAB semi-clathrates formed from gas mixtures containing CO.

Ye et al. (*32*) conducted experiments on semi-clathrates that were formed in the presence of two promoters (TBAC and TBPC) with and without carbon dioxide (CO_2). The temperature and pressure ranges at which the experiments were carried out were 279.0 to 292.0 K and 0.6 to 4.1 MPa respectively. The author reported that the equilibrium temperatures of TBAC semi-clathrates are higher than that of semi-clathrates formed from TBPC.

Mayoufi et al. (*33*) conducted an experimental study to measure the phase behaviour of semi-clathrates formed from CO_2 + TBPB + water and TBPB + water, for various concentrations of TBPB varying rage of mole fraction from 0 to 0.073. The author concluded that there would be a decrease in formation pressure of CO_2 hydrate when TBPB is added to water at a low concentration such as 0.0058 mole fraction.

Li et al. (*34*) experimentally investigated the hydrate formation rate and separation effect on the capture of CO_2 from a binary mixture of (CO_2/N_2) by forming a semi-clathrate with 5 wt.% TBAB. The CO_2 recovery (R) was calculated using the expression below,

$$R = \frac{n_{CO_2}^{H}}{n_{CO_2}^{Feed}}$$

where, $n_{CO_2}^{H}$ is denoted as the number of moles of CO_2 in hydrate phase and $n_{CO_2}^{Feed}$is denoted as number of moles of CO_2 in the feed gas. The CO2 recovery was reported as 45% at a feed pressure range (4.30-7.30) MPa.

Mayoufi et al. (*41*) experimentally investigated the equilibrium and dissociation enthalpies of semi-clathrate formed from systems (CO_2 + TBACL + H_2O), (CO_2 + $TBANO_3$ + H_2O) and (CO_2 + TBPB + H_2O). The authors concluded that semi-clathrates formed from TBPB can store two to four times more CO_2 per water molecules, when compared with the other two semi-clathrates formed from TBACL and $TBNO_3$.

Belandria et al. (*42*) experimentally measured the dissociation pressure of semi-clathrate of TBAB formed from the gas mixture carbon dioxide (CO_2) and nitrogen (N_2). The authors observed that the experimental dissociation pressures were lower for the formation of the semi-clathrates when compared with the gas hydrate at the same temperature. The experimental pressure was also seen to decrease as the concentration of the nitrogen gas was increased. The author also observed that when the concentration of the nitrogen gas was increased the pressure required for the formation of the semi-clathrate also increased.

Mohammadi et al. (*43*) measured the phase equilibrium condition of semi-clathrates of TBAB formed in the presence of gas mixture of carbon dioxide and nitrogen ($CO_2 + N_2$). The study was carried out over a temperature range of 277.1 K to 293.2 K and at pressures up to 16.21 MPa. The authors concluded that using TBAB as a promoter contributes more efficiency in separation of CO_2 when compared with conventional hydrate forming technique.

Li et al. (*44*) conducted an experimental study on the equilibrium hydrate formation condition for TBAB semi-clathrates formed with a gas mixture of CO_2 (carbon dioxide) and H_2 (hydrogen). The experiments were carried out over a temperature range of (274.05 to 288.55) K and a pressure range of (0.25 to 7.26) MPa. The author concluded that the equilibrium hydrate formation pressure of semi-clathrates of $CO_2 + H_2 +$ TBAB system is lower when compared with that of the hydrate mixture $CO_2 + H_2$, at the same temperature.

Kim et al. (*53*) studied the effect of the TBAB as promotor on the separation of the CO_2 (carbon dioxide) from a carbon dioxide and hydrogen (CO_2/H_2) gas mixture by the process of hydrate crystallization. The author observed that at a TBAB concentration more than 3.0 mole% the experimental pressure and temperature increased.

Meysel et al. (*52*) experimentally investigated the equilibrium conditions of TBAB semi-clathrates formed from gas mixtures of carbon dioxide and nitrogen ($CO_2 + N_2$). The experiment was carried out between a temperature range of (281 to 290) K and a pressure range of (1.9 to 5.9) MPa. The author concluded that the pressure required for the formation of the semi-clathrates decreased with the increase in the TBAB concentration.

1.8.2 Separation of methane

Methane is a greenhouse gas that is believed to contribute more than 16% of the global greenhouse gas effect. The greenhouse effect of the methane is more than 20 times greater than

that of CO_2 (*24*). The sources that contributes to the emission of methane are natural gas streams, landfills, animal wastes, hydropower reservoirs and coal mining (*24*). Recently the emission of CH_4 from industrial gases have attracted more attention like that paid to the separation of CO_2 using hydrate crystallization. Separation of CH_4 by hydrate crystallization is termed as a novel separation process. Table 1.4 below summarizes the relevant experimental study conducted on CH_4 semi-clathrates.

Table 1.4: Experimental studies on semi-clathrate hydrate for methane systems in combination with hydrate promoters

Author(s)	System	Aim of study
Zhong et al (*54*)	$CH_4 + N_2 + O_2$ + TBAB	Dissociation conditions. Composition of vapour phase.
Sun et al (*55*)	CH_4 + TBAC	Dissociation conditions.
Sun et al (*56*)	CH_4 + TBAB	Dissociation conditions.
Sun et al (*57*)	$CH_4 + N_2$ +TBAB	Gas storage capacity.
Acosta et al (*58*)	$CH_4 + CO_2$ + TBAB	Dissociation conditions. Gas storage capacity.
Fan et al (*59*)	$CH_4 + CO_2$ + TBAB $CH_4 + CO_2$ + TBAC $CH_4 + CO_2$ + TBAF	Dissociation conditions. Composition of vapour phase.
Zhang et al (*60*)	$CH_4 + N_2 + O_2$ + THF	Hydrate composition.
Kondo et al (*61*)	$CH_4 + C_2H_6 + C_3H_8$ + THF	Dissociation conditions.
Ma et al (*63*)	$CH_4 + N_2 + O_2$ + TBAB	Dissociation conditions. Composition of vapour phase.

Summary of the literature review of Table 1.4:

Zhong et al. (*54*) experimentally investigated the equilibrium conditions of semi-clathrates of TBAB formed from gas mixtures of methane, nitrogen and oxygen ($CH_4/N_2/O_2$). The experiments were carried over a temperature range of (282 to 290) K and with a pressure range of (0.99 to 6.56) MPa. The author concluded that the semi-clathrate formation pressure decreases as the TBAB concentration in the solution was increased at a given temperature.

Fan et al. (*59*) experimentally studied the hydrate equilibrium data for the systems ($CO_2 + CH_4 + H_2O$), ($CO_2 + CH_4 + TBAB + H_2O$), ($CO_2 + CH_4 + TBAC + H_2O$) and ($CO_2 + CH_4 + TBAF + H_2O$) at a temperature and pressure range of (280 to 293) K and (0.61 to 69.45) MPa respectively. The author reported that TBAF is the best of the promoters, relative to gas hydrates.

Acosta et al. (*58*) experimentally measured the thermodynamic equilibrium condition of TBAB semi-clathrates formed from gas mixtures of carbon dioxide and methane ($CO_2 + CH_4$). The experiments were carried out in a pressure and temperature range of (286 to 293) K and (3 to 6.5) MPa, respectively. The authors concluded that as the TBAB concentration increases, the pressure required to form a semi-clathrate decrease at a given temperature.

1.8.3 Separation of Hydrogen (H_2)

The ability to store large volume of gas in hydrate form has made hydrate crystallization technique a potentially attractive process for storage and transportation of hydrogen. The conditions required for forming gas hydrates in the presence of hydrogen can be extreme in pressure. However, the addition of quaternary ammonium salts can greatly reduce the pressure required to enclathrate a gas mixture. The Table 1.5 below shows some of the experimental studies that were carried out for the separation of H_2 (hydrogen)

Table 1.5: Experimental studies on semi-clathrate hydrate for hydrogen systems in combination with hydrate promoters

Author(s)	System	Aim of study
Fujisawa et al (*65*)	H_2+TBAB H_2+TBPB H_2+TBAC	Dissociation conditions. Crystal structure was studied using Raman spectroscopic

Author(s)	Gas System	Aim of study
Du et al (*66*)	H_2+$TBANO_3$	Raman spectroscopic studies. Dissociation conditions.
Hashimoto et al (*67*)	H_2+TBAB	Dissociation conditions.
Hashimoto et al (*68*)	H_2+TBAB H_2+THF	Dissociation conditions. Crystal structure was studied using Raman spectroscopic
Karimi et al (*69*)	H_2+TBAOH	Dissociation conditions.
Deschamps et al (*70*)	H_2+TBAB H2+TBPB H2+TBAC	Dissociation conditions.

Summary comments from the literature review of Table 1.5:

Hashimoto et al. (*64*) conducted an experimental study on the thermodynamic stability of semi-clathrates of hydrogen and TBAB for various concentration of TBAB with a varying range of mole fraction from (0.006 to 0.070). The author used Raman spectroscopy to study the structure of the semi-clathrates of TBAB formed from hydrogen gas (H_2) and concluded that only the empty small cage of TBAB semi-clathrates were occupied by H_2 molecules.

Fujisawa et al. (*65*) investigated the thermodynamic stability of semi-clathrates of H_2 (hydrogen) when TBPB is used as a promoter. The temperature and pressure at which the experiments were carried out were between the range of (281.90-295.94) K and (75 to 120) MPa. The author used Raman spectroscopy to study the semi-clathrate crystal structure and concluded that the entrapped H_2 molecules are only present in the small cage.

Du et al. (*66*) experimentally measured the phase equilibrium and dissociation enthalpies of $TBANO_3$ semi-clathrates formed from H_2 (hydrogen). The author concluded that as the concentration of $TBANO_3$ was increased the experimental temperature increased and the experimental pressure decreased for the formation of the semi-clathrates.

Hashimoto et al. (*67*) investigated the thermodynamic stability and H_2 occupancy of semi-clathrates of TBAB and hydrogen. The author studied the crystalline structure of the semi-clathrates using Raman spectroscopy and concluded that at a pressure of 15 MPa and observed that the structure of the hydrate changed from tetragonal to another different structure at a pressure

and temperature 95 MPa and 292 K respectively. The author concluded that after the structural transition the occupied amount of the H_2 in the semi-clathrate increased.

Karmi et al. (*69*) experimentally measured the phase equilibrium and the hydrogen storage capacity of semi-clathrates formed from the system (H_2+ TBAOH+H_2O). The experiment was carried out at a temperature range of 273.15 to 303.15 K and the TBAOH concentration range was between 0.0083 to 0.0323 mole percent. The author reported that even though the H_2 storage capacity did not meet the required condition. However, when compared with the conventional storage method, the current technology was considered a good replacement.

1.9 Review of semi-clathrate phase equilibrium models

This section discusses about the handful of thermodynamic models that have been developed to predict the dissociation condition of semi-clathrates. Since all the existing models for semi-clathrate thermodynamics are based upon the thermodynamic model for gas hydrate formation (i.e. the model of van der Waals and Platteeuw) this model will first be reviewed.

Any thermodynamic model that has been developed to predict the dissociation condition of gas hydrates or semi-clathrates must meet certain condition for the phase equilibrium in the solid-liquid-vapour system (*6*). The conditions that must be satisfied are the pressure and temperature in all the three phase must be equal, chemical potential or the fugacity of each component in all the phase must be equal and the Gibbs free energy must be minimum (*6*).

1.9.1 The Model of van der Waals & Platteeuw for computing the Chemical Potential of Water in a Gas Hydrate

The chemical potential of water in the solid hydrate phase, and subsequently in the solid semi-clathrate, is most commonly computed using the statistical thermodynamic model of van der Waals and Platteeuw (*74*). The mathematical treatment of van der Waals and Platteeuw will be presented in a later section; this section will instead give a contextual overview of the thermodynamic model.

The statistical thermodynamic model of van der Waals and Platteeuw is based upon the following five assumptions:

1. The gas in the cage rotates and vibrates freely.
2. Only one guest molecule can be trapped in each cavity

3. There is no interaction between the entrapped guest molecules
4. Cavities are assumed to be spherical
5. The guest molecules are assumed to be small enough to prevent altering the hydrate lattice.

In their original treatment, van der Waals and Platteeuw used the Lennard-Jones-Devonshire was used by Van der Waals and Platteeuw to calculate the Langmuir constants; these constants represent the interaction between the gas molecule and water molecules in the crystalline structure (*75*). The author reported dissociation pressure of nine different gases at 273 K in literature (*75*).

Subsequently, in 1972, Parrish and Prausnitz (*76*) made minor modifications to the original model of van der Waals and Platteeuw. In particular, Parrish and Prauznitz used the Kihara potential model to calculate the guest and host molecule interaction. The gas phase fugacity was computed with the Redlick-Kwong EOS (*77*). Finally, in 1980, Holder et al. (*78*) reformulated the original equations of van der Waals and Platteeuw in such a way as to eliminate the need for a reference hydrate. The model of van der Waals and Platteeuw, along with the modifications of Parrish and Prausnitz as well as Holder et al. remain the standard for computing hydrate phase equilibrium. Additionally, these equations form the basis for the thermodynamic models that are used to compute phase equilibrium in semi-clathrates.

1.9.2 Models to calculate phase equilibria of semi-clathrates of hydrates

In the last decade, a handful of models have been developed in order to correlate the phase equilibrium of the semi-clathrate hydrates. The first model that was developed was done by Mohammadi et al. (*79*) who proposed a model that is based on artificial neural networks which predicted the dissociation condition for pure hydrate and semi-clathrate system. Even though the values predicted by the model were in acceptable term, it was not clear how the model could be used in the presence of gases other than those for which its parameters were regressed.

Joshi et al. (*80*) developed a thermodynamic model to describe the phase equilibrium of TBAB semi-clathrates formed in the presence of pure CH_4, CO_2 and N_2. The model developed by the author was based on the thermodynamic approach that was developed by Chen and Guo (*81, 82*) for predicting the phase equilibrium of the clathrate hydrate systems. The model of Joshi et al. (*80*) was based on the assumptions that semi-clathrate formation is of a two-step process, where

the first step involves in the formation of the semi-clathrate and the second step involves the adsorption of the guest molecules into the cages of the semi-clathrate. The model was able to predict reasonable results with pure gases however; the semi-empirical nature of the model prevents it from being easily used in the presence of gas mixtures.

Babau et al. (*85*) developed a model based on the model developed by Joshi et al (*80*). The model was developed to predict dissociation condition of semi-clathrate of TBAB formed from argon. The model requires 9 adjustable parameters to predict the dissociation condition of the semi-clathrate. The authors made no attempt to apply their model to describing semi-clathrates formed in the presence of gas mixtures.

A model was proposed by Eslamimanesh (*86*) to describe the phase equilibrium of TBA semi-clathrates formed with pure CO_2, CH_4, N_2 and TBAB. The author used the vdWP theory to describe the hydrate phase. In order to calculate the Langmuir constants, the author used the empirical correlation, similar to that presented by Parrish and Prauznitz (*76*). To determine the fugacity coefficient of the vapour phase, the author used the Peng Robinson EOS (*87*) combining it with Mathias Copeman alpha function [*88*]. The Non-Random Two-Liquid (NRTL) activity model was used to determine the activity coefficient of water and activity coefficient of TBAB was calculated by an empirical correlation. While this model has been subsequently used by several other research groups it suffers from the requirement of a large number of adjustable parameters as well as a completely empirical correlation for the vapour pressure of the solid salt, which is physically nonsensical. The large number of parameters and empirical correlations means that the model of Eslamimanesh (*86*) cannot be extended to describing the thermodynamics of semi-clathrates formed in the presence of mixed gases.

Liao et al. (*83*) developed a thermodynamic model to describe the phase behaviour of the semi-clathrate hydrate of TBAB formed fin the presence of pure CH_4, CO_2, N_2 and gas mixtures of ($CO_2 + N_2$, $CH_4 + N_2$). The model proposed by the author is similar to that developed by Joshi et al. (80) in that it is based on the work of Chen and Guo (*92, 93*). The author used Patel Teja (*84*) EOS, to calculate the fugacity in the vapour phase and the empirical correlation proposed by Elamimanesh et al. (*86*) was used to calculate the activity coefficient of the TBAB. When applying their model to describing the thermodynamics of TBAB semi-clathrates formed in the presence of gas mixtures, the authors treated the gas mixture as a pseudo-pure component rather than

presenting a generalized method for working with gas mixtures. The author reported the average relative deviation ranges from 5% to 9%.

Shi and Liang (*89*) proposed a thermodynamic model that was similar to that of the model proposed by Eslamimanesh (*86*). The author used the vdWP theory to describe the hydrate phase. The fugacity in vapour phase was calculated by Peng-Robinson EOS and eNRTL (electrolyte Non Random Two Liquid) was used to calculate the activity coefficient in the aqueous phase (*86*). As was the case with the original work of Eslamimanesh (*86*), the model of Shi and Liang (*89*) is not extendable to gas mixtures. The average relative deviation reported for this model is in the range of (5-12) %.

Paricaud (*90*) developed a thermodynamic model, based on reaction equilibrium, to correlate the equilibrium conditions of TBAB semi-clathrate of TBAB formed from CO_2 (carbon dioxide). The author has used SAFT-VRE (Statistical associating fluid theory with variable range of electrolyte) for modelling all fluid phase. The semi-clathrate to hydrate phase is described by vdWP theory. The author used the empirical correlation developed by Parrish and Prausnitz (*76*) to calculate the Langmuir constant. In this model the three phase equilibrium (Vapour-Liquid-Hydrate) is solved at a given pressure to determine the semi-clathrate dissociation temperature. The average relative deviation reported by the author is 10%.

Fukumoto et al. (*91*) developed a thermodynamic model to predict the dissociation condition of semi-clathrate by applying the principles of the model developed by Paricaud (*90*). The model developed by the author was used to predict the semi-clathrates of CO_2 formed from TBAB, TBAC, TBAF and TBPB. The fluid phase is described by using SAFT-VRE EOS (*92*). An interesting feature of this model is that it was also used to predict the fusion enthalpies.

Kwaterski and Herri (*93*) developed a model based on the model that was similar to that developed by Paricaud (*90*). The model uses SRK (Soave-Redich-Kwong) EOS to determine the fugacity in the vapour phase. The mole fraction of the gas in the liquid phase is calculated by Henry's law and e-NRTL model is used to describe the liquid phase. The hydrate phase is described by the use of vdWP theory. Unlike the model developed by Paricaud (*90*) that uses an empirical correlation to calculate the Langmuir constants, the author used Kihara potential for describing the guest and host molecule interaction in the hydrate structure. While this model showed promise, Garcia (*22*) was not able to duplicate the results. Subsequently, in a private

communication (*22*) Kwaterski conceded that he must have made an error when programming his model.

Another model that was developed based on the model developed by Eslamimanesh (*86*) was developed by Verret et al. (*94*). The Trebble-Bishnoi EOS is used to calculate the fugacity in the vapour phase and e-NRTL to calculate the activity coefficient in the fluid phase. The hydrate phase equilibrium is calculated based on vdWP theory. The %AARE (average absolute error) was reported as 5% and 22% for CO_2 and CH_4 semi-clathrates respectively formed from TBAB. No attempt was made, by the authors, to extend their model to describing gas mixtures.

Garcia et al (*23*) developed a thermodynamic model based on reaction equilibrium, to correlate the equilibrium condition of TBAB and TBAC semi-clathrate formed from (Xe, Ar, CH_4, CO_2, N_2 and H_2). The model uses the PSRK EOS to determine the fugacity in the vapour phase. LIFAC is used to calculate the activity coefficient from the liquid or fluid phase. The hydrate phase is described by the use of vdWP theory. Unlike the model developed by Paricaud (*90*) that uses an empirical correlation to calculate the Langmuir constants, the author used Kihara potential for describing the guest and host molecular interaction in the hydrate structure.

As has been noted in the above literature review, a general thermodynamic model for semi-clathrates in the presence of mixed gases has yet to be presented. In the current work, the modelling approach of Garcia et al. (*23*) is extended to describing such systems. Where parameters are already available, these parameters are used when correlating the equilibrium conditions of semi-clathrates formed from gas mixtures. Thus, the new approach is readily applicable to correlating the equilibrium conditions of semi-clathrates formed in the presence of gas mixtures.

Chapter Two: **Presentation of the thermodynamic model**

This chapter presents a thermodynamic model that is used to correlate the phase equilibrium of the TBAB semi-clathrates formed in the presence of various gas mixture of (CH_4 + N_2) (*58*), (CO_2 + N_2) (*52*), (CO_2 + H_2) (*31*) and (CO_2 + CO + H_2) (*31*). While there is equilibrium data for semi-clathrates formed in the presence of other quaternary ammonium salts and in the presence of gas mixtures, only the data for the previously mentioned mixtures include a measurement of the equilibrium vapour phase composition, which will be required for implementing the new thermodynamic model. The model presented here is based on the reaction equilibrium and the Gibbs energy of minimization is applied to solve the model. As a first step, the model is developed to describe the solid-liquid equilibrium between the salt and water and eventually the model is extended to predict the dissociation temperature of the semi-clathrate hydrate at a given pressure. As a final step, the model is extended to predict the three-phase equilibrium by applying the vdWP (Vander Waals Platteuw) to predict the dissociation temperature of the semi-clathrate formed at a given TBAB concentration and pressure.

2.1 Description of thermodynamic model

In the present section the thermodynamic model developed by Garcia et al. (*23*), which was derived to describe the thermodynamics of semi-clathrate formation in the presence of pure gasses, is extended to describing the thermodynamics of semi-clathrates formed in the presence of mixed gasses. The model of Garcia et al. (*23*) was based on the reaction equilibrium formulation set out by Paricaud (*90*). Garcia et al. (*23*) used Paricaud's model for the chemical potential of water in the solid phase along with the PSRK equation of state for the vapour and liquid phases. The PSRK equation of state uses free-energy mixing rules that allow one to account for the non-ideality of aqueous electrolyte solutions. In particular, the free-energy mixing rules use the LIFAC model to compute the activities, and activity coefficients, of the electrolyte species within the liquid phase. It should be noted that for non-electrolytes, the LIFAC model simplifies to the well-known UNIFAC model. As will be shown, extending the model of Garcia et al. (*23*) to gas mixtures occurs via the free-energy mixing rules.

The model of Garcia et al. (*23*) contains two adjustable parameters for each semi-clathrate structure plus three Kihara potential parameters for each pure gas component. For all but one of the gasses that will be encountered in the present study (CO) these parameters were regressed by Garcia et al. (*23*) and will be used in the present study. Beyond the aforementioned parameters, the only equation of state binary interaction parameters, most of which are already available, will be needed for correlating the equilibrium conditions of TBAB semi-clathrates formed in the presence of mixed gasses.

In this section, a generalized formulation of the model of Garcia et al. (*23*) is presented. The model is formulated in two steps; in the first step, the model for describing the liquid-solid equilibria is introduced. Subsequently, the developed liquid-solid model is combined with the van der Waals & Platteeuw theory in order to describe three-phase equilibrium in systems containing semi-clathrates. The liquid-solid equilibrium model was developed in order to regress parameters related to the solid semi-clathrate structure. The subsequent step, which is based on a reaction equilibrium formulation, is subsequently used for correlating the three-phase equilibrium data for TBAB semi-clathrates formed in the presence of mixed gasses.

2.1.1 ***Solid-Liquid equilibrium***

Garcia et al. (*23*) adopted the Solid-Liquid phase reaction equilibrium approach of Paricuad (*90*) in order to obtain thermodynamic parameters related to the empty, crystalline, semi-clathrate structure. While the necessary parameters have already been regressed by Garcia et al. (*23*), this development is being repeated, in the present work, for the sake of supporting subsequent material.

Garcia et al. (*23*) envisioned the formation and decomposition dissociation of a semi-clathrate, in a binary solution consisting of a single salt (*CA*) and water, as a combined chemical reaction, which is written as:

$$C_{\nu_c}A_{\nu_a} \cdot \nu_w H_2O(H) \rightleftharpoons \nu_w H_2O(L) + \nu_c C^{z_c^+}(L) + \nu_a A^{|z_a^-|}(L) \qquad \textbf{(2.1)}$$

Where z_a^- And z_c^+ are the total charge of the anion and cation, respectively. The ν_a and ν_c are the number of anions (*A*) and the number of cations (*C*), respectively. From basic chemical thermodynamics (*114*), the reaction equilibrium constant *K(T)*, which is the standard constant which is used to describe the equilibrium, is expressed as:

$$K(T) = \frac{(a_w^L)^{\nu_w}(a_c^L)^{\nu_c}(a_a^L)^{\nu_a}}{a_h^H} \exp\left(-\frac{1}{RT}\int_P^{P^0} \left(\nu_w V_w^L + \nu_c V_c^{\infty,L} + \nu_a V_a^{\infty,L} - V_h^H\right) dP \right) \quad \textbf{(2.2)}$$

In equation (2.2), the subscript h represents the solid semi-clathrate ($C_{\nu_c}A_{\nu_a} \cdot \nu_w H_2O$), a_h^H is the activity of the semi-clathrate phase, a_w^L is represented as activity of water in liquid phase and a_a^L and a_c^L are the activity of the anion and cation in the liquid phase, respectively. V_w^L and V_h^H are the molar volume of water and semi-clathrate, respectively. Finally, $V_c^{\infty,L}$ and $V_a^{\infty,L}$ are the partial volume of anion and cation at infinite dilution of the salt, respectively.

Since the semi-clathrate phase is a pure solid, rather than a solid solution, the activity of the semi-clathrate is unity.

$$a_h^H = 1 \quad \textbf{(2.3)}$$

In the liquid phase, the activity of the compounds is expressed as a product of mole fraction and activity coefficient. Thus, the activity of water can be written as:

$$a_w^L = x_w^L \gamma_w^L \quad \textbf{(2.4)}$$

The activities of the cation and anion in the liquid phase are given by:

$$a_c^L = x_c^L \gamma_c^L \quad \textbf{(2.5)}$$

$$a_a^L = x_a^L \gamma_a^L \quad \textbf{(2.6)}$$

The LIFAC (*96*), which will be presented in a subsequent section, is used in the present work to determine the activity coefficient in the liquid phase ($\gamma_w^L, \gamma_c^L, \gamma_a^L$). The LIFAC model was chosen because it is also the activity coefficient model that is embedded in the PSRK equation of state's

free energy mixing rules. Substituting equations (2.4), (2.5), and (2.6) into equation (2.2), and we get:

$$\ln K(T) = \nu_w \ln(x_w^L \gamma_w^L) + \nu_c \ln(x_c^L \gamma_c^L) + \nu_a \ln(x_a^L \gamma_a^L) - \frac{1}{RT}\int_P^{P^0} \left(\nu_w V_w^L + \nu_c V_c^{\infty,L} + \nu_a V_a^{\infty,L} - V_h^H\right) dP \quad \textbf{(2.7)}$$

From the standard Gibbs energy of dissociation is related to the chemical equilibrium constant by:

$$\Delta_{dis} G^0(T) = -RT \ln K(T) \quad \textbf{(2.8)}$$

Additionally, for the previously noted reaction the total Gibbs energy of dissociation for the system can be written as (*95, p. 535*):

$$\Delta_{dis} G^0(T) = \sum_i \nu_i \mu_i^0 = \nu_w \mu_w^{0,L} + \nu_c \mu_c^{0,L} + \nu_a \mu_a^{0,L} - \mu_h^{0,H} \quad \textbf{(2.9)}$$

The standard chemical potential of semi-clathrate in the hydrate phase is represented as $\mu_h^{0,H}$. The standard chemical potential of water, cation and anion in liquid phase is represented as $\mu_w^{0,L}$,$\mu_c^{0,L}$, and $\mu_a^{0,L}$. When Equations (2.7), (2.8) and Equation (2.9) are combined we get the following equation below:

$$-\frac{1}{RT}\left(\nu_w \mu_w^{0,L} + \nu_c \mu_c^{0,L} + \nu_a \mu_a^{0,L} - \mu_h^{0,H}\right) = \nu_w \ln(x_w^L \gamma_w^L) + \nu_c \ln(x_c^L \gamma_c^L) + \nu_a \ln(x_a^L \gamma_a^L) - \frac{1}{RT}\int_P^{P^0} \left(\nu_w V_w^L + \nu_c V_c^{\infty,L} + \nu_a V_a^{\infty,L} - V_h^H\right) dP \quad \textbf{(2.10)}$$

The Equation (2.11) and (2.12) represent the chemical potential of the semi-clathrate and of water in liquid phase, respectively.

$$\mu_h^{0,H}(T) = \mu_h^H(T,P) + \int_P^{P^0} V_h^H \, dP \quad \textbf{(2.11)}$$

$$\mu_w^{0,L}(T) = \mu_w^L(T,P) + \int_P^{P^0} V_w^L \, dP \tag{2.12}$$

Equations (2.13) and (2.14), below, represent the chemical potential of the cation, $\mu_c^{0,L}(T)$ and anions, $\mu_a^{0,L}(T)$ (22).

$$\mu_c^{0,L}(T) = \int_P^{P^0} V_c^{\infty,L} \, dP + \left\{ \lim_{x_w \to 1} [\mu_c^L(T,P,x_w) - RT\ln(x_c)] \right\} \tag{2.13}$$

$$\mu_a^{0,L}(T) = \int_P^{P^0} V_a^{\infty,L} \, dP + \left\{ \lim_{x_w \to 1} [\mu_a^L(T,P,x_w) - RT\ln(x_a)] \right\} \tag{2.14}$$

The standard chemical potential of the compound *i* in terms of temperature dependence is expressed in term of the isobaric heat capacity and enthalpy as in the below-mentioned expression.

$$\mu_i^{0,L}(T) = \frac{\mu_i^{0,L}(T_0)}{T_0} + H_i^{0,L}(T_0)\left(\frac{1}{T} - \frac{1}{T_0}\right) - \int_{T_0}^{T} \left(\int_{T_0}^{T'} C_{p,i}^L(T'')dT'' \right) \frac{dT'}{T'^2} \tag{2.15}$$

The isobaric heat capacity of compound *i* in the liquid phase is represented as $C_{p,i}^L$, the standard enthalpy of compound *i* in the liquid phase is represented as $H_i^{0,L}$.The equation (2.15) is applied to all the compounds present in the liquid phase that is cation, anion and water. By applying the equation (2.15), we get the following expression below:

$$\frac{1}{RT_0}\left(\mu_h^{0,H}(T_0) - \nu_w\mu_w^{0,L}(T_0) - \nu_c\mu_c^{0,L}(T_0) - \nu_a\mu_a^{0,L}(T_0)\right)$$
$$+\frac{1}{R}\left(\frac{1}{T}-\frac{1}{T_0}\right)\left(H_h^{0,H}(T_0) - \nu_w H_w^{0,L}(T_0) - \nu_c H_c^{0,L}(T_0)\right.$$
$$\left.-\nu_a H_a^{0,L}(T_0)\right)$$
$$+\frac{1}{R}\int_{T_0}^{T}\left(\int_{T_0}^{T'}\left(\nu_w C_{p,w}^{L}(T'') + \nu_c C_{p,c}^{L}(T'') + \nu_a C_{p,a}^{L}(T'')\right.\right. \quad \textbf{(2.16)}$$
$$\left.\left.-\nu_w C_{p,h}^{H}(T'')\right)dT''\right)\frac{dT'}{T'^2}$$
$$= \nu_w \ln(x_w^L\gamma_w^L) + \nu_c \ln(x_c^L\gamma_c^L) + \nu_a \ln(x_a^L\gamma_a^L)$$
$$-\frac{1}{RT}\int_{P}^{P^0}\left(\nu_w V_w^L + \nu_c V_c^{\infty,L} + \nu_a V_a^{\infty,L} - V_h^H\right)dP$$

The molar quantities ($\Delta_{dis}V^0(T)$,$\Delta_{dis}H^0(T)$, and $\Delta_{dis}C_p^0(T)$) that represents the change in property accompanying the dissociation reaction of the clathrate are defined below in the following equations.

$$\Delta_{dis}H^0(T) = \nu_w H_w^{0,L}(T_0) + \nu_c H_c^{0,L}(T_0) + \nu_a H_a^{0,L}(T_0) - H_h^{0,H}(T_0) \quad \textbf{(2.17)}$$

$$\Delta_{dis}V^0(T) = \nu_w V_w^L + \nu_c V_c^{\infty,L} + \nu_a V_a^{\infty,L} - V_h^H \quad \textbf{(2.18)}$$

$$\Delta_{dis}C_p^0(T) = \nu_w C_{p,w}^L(T) + \nu_c C_{p,c}^L(T) + \nu_a C_{p,a}^L(T) - C_{p,h}^H(T) \quad \textbf{(2.19)}$$

When equations (2.9), (2.17), (2.18), and (2.19) are substituted into equation (2.16), we get the following expression below:

$$\frac{\Delta_{dis}G^0(T)}{RT_0}+\frac{\Delta_{dis}H^0(T)}{RT}\left(1-\frac{T}{T_0}\right)-\frac{1}{R}\int_{T_0}^{T}\left(\int_{T_0}^{T'}\left(\Delta_{dis}C_p^0(T)\right)dT''\right)\frac{dT'}{T'^2}$$
$$=\nu_w\ln(x_w^L\gamma_w^L)+\nu_c\ln(x_c^L\gamma_c^L)+\nu_a\ln(x_a^L\gamma_a^L)$$
$$-\frac{1}{RT}\int_{P}^{P^0}\left(\Delta_{dis}V^0(T)\right)dP \qquad \textbf{(2.20)}$$

By assuming $\Delta_{dis}C_p^0(T)$ and $\Delta_{dis}V^0(T)$ are independent of temperature and pressure, respectively, Equation (2.20) can be rewritten as follows:

$$\frac{\Delta_{dis}G^0(T_0)}{RT_0}+\frac{\Delta_{dis}H^0(T_0)}{RT}\left(1-\frac{T}{T_0}\right)+\frac{\Delta_{dis}C_p^0(T)}{R}\left(1+\ln\left(\frac{T_0}{T}\right)-\frac{T_0}{T}\right)$$
$$+\frac{\Delta_{dis}V^0(T)}{RT}(P-P^0)+\nu_w\ln(x_w^L\gamma_w^L)+\nu_c\ln(x_c^L\gamma_c^L)$$
$$+\nu_a\ln(x_a^L\gamma_a^L)=0 \qquad \textbf{(2.21)}$$

The above equation (2.21) describes the equilibrium conditions between the liquid phase and solid phase and the solid semi-clathrate when the semi-clathrate is formed in the absence of a gas. Garcia et al. (*23*) evaluated equation (2.21) at the congruent melting point, in order to regress the values of the parameter ($\Delta_{dis}G^0(T_0)$) for the solid semi-clathrate. Furthermore, in order to reduce the number of parameters, Paricuad (*90*) and Garcia et al. (*23*) assumed that the value of $\Delta_{dis}C_p^0(T)$ was negligible. The congruent melting temperature is the equilibrium temperature at which the semi-clathrate is dissociated under the atmospheric pressure (P^0) and stoichiometric condition. The stoichiometric conditions of the semi-clathrate phase can be calculated using the following equation below (*22*):

For water:

$$x_w^{(st),H}=x_w^L=\frac{\nu_w}{(\nu_c+\nu_a+\nu_w)} \qquad \textbf{(2.22)}$$

For cations:

$$x_c^{(st),H} = x_c^L = \frac{\nu_c}{(\nu_c + \nu_a + \nu_w)} \quad \textbf{(2.23)}$$

For anions:

$$x_a^{(st),H} = x_a^L = \frac{\nu_a}{(\nu_c + \nu_a + \nu_w)} \quad \textbf{(2.24)}$$

Thus, the value of $\Delta_{dis}G^0(T_0)$ can be obtained when evaluating equation (2.21) at the congruent melting point
$T = T_0; P = P^0$, the value of $\Delta_{dis}G^0(T_0)$ can be obtained:

$$\frac{\Delta_{dis}G^0(T_0)}{RT_0} = -\left(\nu_w \ln\left(x_w^{(st),H}\gamma_w^L\right) + \nu_c \ln\left(x_c^{(st),H}\gamma_c^L\right) + \nu_a \ln\left(x_a^{(st),H}\gamma_a^L\right)\right) \quad \textbf{(2.25)}$$

Once the value of $\Delta_{dis}G^0(T_0)$ had been obtained, Garcia et al. (*23*) used equation (2.21), along with SLE data for the TBAB water system, to regress the values of $\Delta_{dis}H^0(T_0)$ and $\Delta_{dis}V^0(T)$. The values for$\Delta_{dis}G^0(T_0)$, $\Delta_{dis}H^0(T_0)$ and $\Delta_{dis}V^0(T)$ are subsequently used in modeling the equilibrium conditions for semi-clathrates formed in the presence of gases. This is detailed in the next section.

2.1.2 Vapour–liquid-hydrate equilibrium

Paricaud (*90*) adapted the van der Waals and Platteeuw (vdWP) model to predict the equilibrium conditions of the semi-clathrates in the presence of pure gas, or a gas mixture. The vdWP model was originally derived for clathrates, rather than specifically for semi-clathrates; thus, the word "clathrate" will be used in parts the following section. When deriving the chemical potential of the empty clathrate, the following assumptions are assumed as presented by van der Waals and Platteuw and Paricaud (*75*, *90*):

- In the molecular lattice, the position of the host molecule is fixed.
- The gas molecules do not distort the cavities in the lattice.
- Cavities are assumed to be spherical.

- Only one gas molecule can be trapped in a given cavity.
- Neglecting the guest-guest interaction.
- Neglecting the quantum effect.

The chemical potential of the clathrate is expressed by Paricaud (*90*) as, $\mu_h^{H,F}$, is given by the expression below:

$$\mu_h^{H,F} = \mu_h^{H,\beta} + \sum_{i=1}^{N_{cav}} n_i \ln\left(1 - \sum_{j=1}^{N_{gas}} Y_{ij}\right) \quad \textbf{(2.26)}$$

In the above expression (Equation 2.26), chemical potential per salt molecules in the empty metastable phase β is represented as $\mu_h^{H,\beta}$. The number of cavities of type *i* per salt molecule is denoted as n_i , occupancy fraction of cavities *i* is denoted as Y_{ij} for the molecule of type *j*. The equations (2.27) and (2.28) below describes the $\mu_h^{H,\beta}$ and $Y_{ij.}$

$$\mu_h^{H,\beta} = \nu_c \mu_c^{H,\beta} + \nu_a \mu_a^{H,\beta} + \nu_w \mu_w^{H,\beta} \quad \textbf{(2.27)}$$

$$Y_{ij} = \frac{C_{ij}\hat{f}_j}{1 + \sum_{j=1}^{N_{gas}} C_{ij}\hat{f}_j} \quad \textbf{(2.28)}$$

The Langmuir constant and the fugacity of molecule *j* in the mixture are represented as C_{ij} and $\hat{f}_j$respectively. The fugacity in the present study is calculated by PSRK EoS. In equation (2.28), the fugacity is taken to be the vapour phase fugacity; at equilibrium, this is appropriate because the fugacity of each component, in each phase, is equal. Also note that the fugacity is an implicit function of the gas phase composition.

Assuming the Langmuir constants are only a function of temperature, and that the cavities entrapping the gas molecules are spherical, the C_{ij} can be defined by the equation (2.29) (*97*):

$$C_{ij} = \frac{4\pi}{kT}\int_0^{R_{cell-a_i}} e^{-w(r)/kT} r^2 dr \quad \textbf{(2.29)}$$

In the above equation (2.29), *k* is the Boltzmann's constant, R_{cell} is the radius of the cavity, a_i is the radius of spherical core of component *i*, r is the distance of the guest molecule from the center of the cavity, and the potential function for the interaction between the guest molecule and molecule constituting the cavity is denoted as $w(r)$ (*98*). Usage of the Kihara potential function (*99, 100*) was suggested by McKoy and Sinanogly (*101*) to describe interaction of the guest molecule and the water molecules. Equations (2.30 and 2.31) represents the guest molecule-cavity interaction using the Kihara potential.

$$w(r) = 2z\varepsilon\left[\frac{\sigma^{12}}{R_{cell}^{11}\cdot r}\left(\delta^{10} + \frac{a}{R_{cell}}\delta^{11}\right) - \frac{\sigma^{6}}{R_{cell}^{5}\cdot r}\left(\delta^{4} + \frac{a}{R_{cell}}\delta^{5}\right)\right] \quad \textbf{(2.30)}$$

$$\delta^N = \frac{\left(1 - \frac{r}{R_{cell}} - \frac{a}{R_{cell}}\right)^{-N} - \left(1 + \frac{r}{R_{cell}} - \frac{a}{R_{cell}}\right)^{-N}}{N} \quad \textbf{(2.31)}$$

In the above equations (2.30 and 2.31) the coordination number of the cavity is represented as *z*. The radius of the spherical molecule core, collision diameter, and minimum energy is represented as *a*, σ and ε respectively. The Kihara potential parameters (*a*, σ and ε) are regressed using the hydrate phase equilibrium data. The subscript *N* can take the values of 4,5,10 or 11.

Equations (2.26) through (2.31) were originally applied to clathrate hydrates. In order to extend this analysis to semi-clathrates, Paricaud (*90*) considered the equilibrium condition of the reaction given by equation (2.1).

At equilibrium, the Gibbs free energy is minimum (dG=0). Hence during the dissociation reaction the equilibrium condition for the three-phase system (S-L-V) can be expressed in terms of change in the Gibbs free energy. The dissociation reaction is expressed by Equation (2.32) written below:

$$\Delta_{dis}G = \sum_i \nu_i\mu_i \;\; = \nu_w\mu_w^L + \nu_c\mu_c^L + \nu_a\mu_a^L - \mu_h^H \quad \textbf{(2.32)}$$

When equations (2.26), (2.12),(2.13),and (2.14) are substituted into equation (2.32), it leads to the following equation that is expressed below:

$$\frac{\Delta_{dis}G^0(T)}{RT} = \frac{1}{RT}\left(\nu_w\mu_w^{0,L}(T) + \nu_c\mu_c^{0,L}(T) + \nu_a\mu_a^{0,L}(T) - \mu_h^{H,\beta}(T)\right)$$
$$-\frac{1}{RT}\int_P^{P^0}\left(\nu_w V_w^L + \nu_c V_c^{\infty,L} + \nu_a V_a^{\infty,L} - V_h^H\right)dP + \nu_a \ln(x_a^L\gamma_a^L) \qquad \textbf{(2.33)}$$
$$+\nu_w \ln(x_w^L\gamma_w^L) + \nu_c \ln(x_c^L\gamma_c^L) - \sum_{i=1}^{N_{cav}} n_i \ln\left(1 - \sum_{j=1}^{N_{gas}} Y_{ij}\right) = 0$$

Assuming $\Delta_{dis}C_p^0(T)$ and $\Delta_{dis}V^0(T)$, eq(2.18 & 2.19) are temperature and pressure independent respectively and evaluating each and every chemical potential term present in eq (2.33) using eq (2.15) the following expression is obtained (*90*).

$$\frac{\Delta_{dis}G^0(T)}{RT} = \frac{\Delta_{dis}G^0(T_0)}{RT_0} + \frac{\Delta_{dis}H^0(T_0)}{RT}\left(1 - \frac{T}{T_0}\right) + \frac{\Delta_{dis}V^0(T_0,P^0)}{RT}(P - P^0)$$
$$+\nu_w \ln(x_w^L\gamma_w^L) + \nu_c \ln(x_c^L\gamma_c^L) + \nu_a \ln(x_a^L\gamma_a^L) \qquad \textbf{(2.34)}$$
$$-\sum_{i=1}^{N_{cav}} n_i \ln\left(1 - \sum_{j=1}^{N_{gas}} Y_{ij}\right) = 0$$

Equation (2.34) is the final expression that has to be computed to solve for the given pressure to predict the dissociation temperature of the semi-clathrate. In the above expression, Y_{ij} and activity coefficient are nonlinear functions of temperature. For the semi-clathrate formed from TBAB, the value of n_i is 3 (*22*). Table 3.1 summarizes the stoichiometric coefficient for TBAB ion constituents in our present study.

Table 2.1: Summary of stoichiometric coefficients for TBAB ion constituents used in the present work (22).

Salt	TBAB
Cation	TBA^+
Anion	Br^-
ν_w	38
ν_c	1
ν_a	1

2.2 PSRK EQUATION OF STATE

The Predictive-Soave-Redlich-Kwong equation of state (PSRK), which was originally presented by Holderbaum and Gmehling (*105*) is based on the Soave-Redlich-Wong (SRK) (*106*) equation of state. The pressure-explicit form of the PSRK equation of states is given by the following:

$$P = \frac{RT}{v-b} - \frac{a}{v(v+b)} \tag{2.35}$$

Where *P* is the pressure, *T* is the temperature, *v* is the molar volume, *a* is a term that relates attractive energy, and b is the repulsive term. Equation (2.35) appears to be identical to the SRK equation of state. Where PSRK departs from the SRK equation of state is by modifications that are made to the *a* and *b* terms, that were made in order to make PSRK suitable for vapour-liquid equilibria of polar as well as non-polar mixtures.

The first modification is related to the temperature dependence of the pure component parameter a_i, which was the only function of the acentric factor ω in the original SRK EoS (Soave, 1972). These original equations are presented below:

$$a_i = 0.42748 \frac{\left(RT_{c,i}\right)^2}{P_{c,i}} f(T) \tag{2.36}$$

$$f(T) = \left[1 + c_1\left(1 - T_{r,i}^{0.5}\right)\right]^2 \tag{2.37}$$

$$c_1 = 0.48 + 1.574\omega_i - 0.176\omega_i^2 \tag{2.38}$$

$$T_{r,i} = \frac{T}{T_{c,i}} \tag{2.39}$$

In the above equations, R is the universal gas constant, $T_{c,i}$, $P_{c,i}$, and ω_i are the critical temperature, critical pressure and acentric factor of i compound, respectively. In order to improve the equation of state's accuracy when applied to polar components, the expression proposed by Mathias and Copeman constant (*107*) is employed in the PSRK equation, instead of equation (2.37):

$$f(T) = \left[1 + c_1\left(1 - T_{r,i}^{0.5}\right) + c_2\left(1 - T_{r,i}^{0.5}\right)^2 + c_3\left(1 - T_{r,i}^{0.5}\right)^3\right]^2 \; T_r < 1 \tag{2.40}$$

$$f(T) = \left[1 + c_1\left(1 - T_{r,i}^{0.5}\right)\right]^2 \; T_r > 1 \tag{2.41}$$

The constants c_1, c_2, and c_3 are adjustable parameters regressed from vapour pressure experimental data. These constants are available in Holderbaum and Gmehling (Holderbaum & Gmehling, 1991).

The second modification with PSRK EoS is in the use of free energy mixing rules for a; The free energy mixing rule for a is based on the work by Michelsen. The general principle of the chosen free energy mixing rules is that an activity coefficient model and an equation of state produce the same value for the excess Gibbs energy at a reference pressure:

$$\frac{g^{E,EoS}}{RT} = \frac{g^{E,\gamma}}{RT} \; (P = P^{ref}) \tag{2.42}$$

In equation (2.42), $g^{E,EoS}$ and $g^{E,\gamma}$ are the Excess Gibbs energy calculated from an EoS, and an activity coefficient model, respectively. After applying Equation (2.42) to the original SRK EoS, along with the thermodynamic definition of the excess Gibbs Free energy, the following expressions for a and b are obtained:

$$a = bRT\left(\frac{1}{A_1}\frac{g^E}{RT} + \sum_i x_i \frac{a_i}{b_i RT} + \frac{1}{A_1}\sum_i x_i ln\left(\frac{b}{b_i}\right)\right) \tag{2.43}$$

$$\frac{g^E}{RT} = \sum_i x_i ln\gamma_i \tag{2.44}$$

$$b = \sum_i x_i b_i \tag{2.45}$$

$$b_i = 0.08664 \frac{RT}{P_{c,i}} \quad \textbf{(2.46)}$$

In equation (2.43), A_1 is a constant whose value is -0.64663, x_i is the mole fraction of component i, γ_i is the activity coefficient of component i, which is calculated with the LIFAC activity coefficient model. The LIFAC model will be covered in detail in a subsequent section. However, at this point, it should be noted that the LIFAC model reduces to the UNIFAC model for pairs of uncharged species.

Table 2.2: Critical constants of CH_4, CO_2, N_2, H_2, CO, and H_2O required in the PSRK model (*22*)

Component	P_c/ MPa	T_c / K	Acentric factor/ ω	c_1	c_2	c_3	MW / g·mol^{-1}
CH_4	4.5992	190.564	0.0114	0.4926	0	0	16.043
CO_2	7.3773	304.128	0.2236	0.8252	0.2515	-1.7039	44.009
N_2	3.3958	126.192	0.0372	0.5427	0	0	28.014
CO	3.48	132.9	0.049	0.5567	0	0	28.01
H_2	1.315	33.19	-0.2187	0.1252	0	0	2.016
H_2O	22.064	647.096	0.3443	1.0783	-0.5832	0.5464	18.015

2.3 UNIFAC method

As previously noted, for the uncharged species, the activity coefficients that are needed in the free energy mixing rules are computed from the UNIFAC model. The UNIFAC method (*109*) was developed by Fredenslund et al. (*109*) to predict the activity coefficients in nonelectrolyte mixtures. The UNIFAC method combines the functional-group concept with a model for activity coefficients based on an extension of the quasi-chemical theory of liquid mixtures (UNIQUAC) (*110*). Due to the predictive nature of the method, it can be used in cases where there are no experimental data available for regressing the interaction parameters needed in other models.

The first parameters to be computed are the Group Volume (R_k) and Surface Area (Q_k), which are parameters characteristic of each group. Once the value of these parameters is known, the volume contribution of each molecule can be calculated using Equation (2.47).

$$r_i = \sum_k v_k^{(i)} R_k \quad \textbf{(2.47)}$$

Correspondingly, the surface fractions are determined by means of Equation (2.48).

$$q_i = \sum_k v_k^{(i)} Q_k \quad \textbf{(2.48)}$$

Table 2.3: Molecular and group parameters for UNIFAC and LIFAC (*22*)

Component	group	$v_k^{(i)}$	R_k	Q_k
CH_4	CH_4	1	1.129	1.124
CO_2	CO_2	1	1.3	0.982
N_2	N_2	1	0.856	0.93
H_2	H_2	1	0.416	0.571
CO	CO	1	0.7110	0.8280
Water	H_2O	1	0.92	1.4
TBAB	CH_3	4	0.9011	0.848
	CH_2	12	0.6744	0.54
	N^+	1	3.0	3.0
	Br^-	1	1.2331	1.1510

The variable $v_k^{(i)}$ can be thought of as representing the number of times that group *k* is present in the molecule *i*. These two parameters, r_i and q_i, do not depend on the composition; they only depend upon the structure of a given molecule. The values of (Q_i, q_i) are used to determine the matrix $e_{k,i}$, which contains the surface fraction of each group in each molecule as shown below:

$$e_{k,i} = \frac{v_k^{(i)} Q_k}{q_i} \quad \textbf{(2.49)}$$

The surface area fraction for each group in the mixture, θ_k, is found from:

$$\theta_k = \frac{\sum_i x_i q_i e_{k,i}}{\sum_j x_j q_j} \quad \textbf{(2.50)}$$

Interaction parameters between groups ($a_{m,k}, b_{m,k}, c_{m,k}$) are taken from the UNIFAC tables (*109*) and are used to calculate the variable $\tau_{m,k}$*:*

$$\tau_{m,k} = exp\left[-\frac{a_{m,k} + b_{m,k}T + c_{m,k}T^2}{T}\right] \quad \textbf{(2.51)}$$

This variable is used to determine:

$$\beta_{i,k} = \sum_m e_{mi}\tau_{m,k} \quad \textbf{(2.52)}$$

$$s_k = \sum_m \theta_m \tau_{m,k} \quad \textbf{(2.53)}$$

The penultimate steps in computing the activity coefficients are to determine the volume and surface area contributions for the molecules, J_i and L_i:

$$J_i = \frac{r_i}{\sum_j x_j r_j} \quad \textbf{(2.54)}$$

$$L_i = \frac{q_i}{\sum_j x_j q_j} \quad \textbf{(2.55)}$$

Finally, the activity coefficients can be computed as the sum of the combinatorial and residual part of the activity coefficient model, as presented below:

$$ln(\gamma_i^C) = 1 - J_i + ln(J_i) - 5q_i\left[1 - \frac{J_i}{L_i} + ln\left(\frac{J_i}{L_i}\right)\right] \quad \textbf{(2.56)}$$

$$ln(\gamma_i^R) = q_i\left[1 - \sum_k\left(\theta_k\frac{\beta_{i,k}}{s_k} - e_{k,i}ln\left(\frac{\beta_{i,k}}{s_k}\right)\right)\right] \quad \textbf{(2.57)}$$

$$ln(\gamma_i) = ln(\gamma_i^R) + ln(\gamma_i^C) \quad \textbf{(2.58)}$$

Extension of PSRK to electrolytes

The PSRK equation of state can be extended to systems containing charged species by choosing an appropriate activity coefficient model for use in the free-energy mixing rules. Basically, the PSRK can be used without any further modification in the vapour phase by assuming that electrolytes are not present in the vapour phase. For the liquid phase, Equation (2.43), Equation (2.44), and Equation (2.45) are changed to:

$$a = bRT\left(\frac{1}{A_1}\frac{g^E}{RT} + \sum_i x_i' \frac{a_i}{b_i RT} + \frac{1}{A_1}\sum_i x_i' ln\left(\frac{b}{b_i}\right)\right) \quad \textbf{(2.59)}$$

$$b = \sum_i x_i' b_i \quad \textbf{(2.60)}$$

$$\frac{g^E}{RT} = \sum_i x_i' ln\gamma_i \quad \textbf{(2.61)}$$

Where x_i' is the salt-free liquid-phase mole fraction of component *i* (gas or solvent). This is appropriate for the computation of *a* and *b* in the liquid phase because the critical properties such as P_c and T_c of the ions are not available. As per the suggestion of Gmehling and Holderbaum (*111, 112, 113*), the LIFAC model is used to compute the activity coefficients in the ionic solution. The LIFAC model is also based on the group contribution concept, and can be used to predict vapour-liquid equilibria in electrolyte solutions.

2.4 LIFAC model

When a salt, such as TBAB, dissociates into its constituent ions in a liquid solvent, three possible types of interaction can occur: solvent-solvent, ion-solvent, and ion-ion. These interactions strongly influence the thermodynamic properties of the system. In the LIFAC model

(*96*), several interactions are considered for computing the excess Gibbs free energy, as shown below:

$$G^E = G^E_{LR} + G^E_{MR} + G^E_{SR} \tag{2.62}$$

G^E_{LR} represents the long range (*LR*) electrostatic forces between the charged species (ions). G^E_{MR} represents the contribution from the charge-dipole interactions as well as the charge-induced dipole interactions. G^E_{SR} represents the short range (*SR*) interactions, and it is described using the UNIFAC method [*109*]. Finally, G^E represents the excess Gibbs free energy of the system. In the case of the solvent, the activity coefficient of the long-range contribution is given by the following expression [96]:

$$\ln \gamma^{LR}_{solv,s} = \frac{2AM_s d}{b^3 d_s}\left[1 + bI^{0.5} - \left(1 + bI^{\frac{1}{2}}\right)^{-1} - 2\ln(1 + bI^{0.5})\right] \tag{2.63}$$

The activity coefficient of the long-range contribution for ion *j* is given by [96]:

$$\ln \gamma^{LR}_{ion,j} = \frac{2AM_s d}{b^3 d}[1 + bI^{0.5} - (1 + bI^{0.5})^{-1} - 2\ln(1 + bI^{0.5})] \tag{2.64}$$

In the above equation, M_s is the molecular weight of the solvent, I is the ionic strength, d_s is the molar density of the solvent s (calculated from DIPPR tables), d is the density of the solvent mixture, and A and b the Debye-Huckel parameters, which are calculated as (*96*):

$$A = 1.327757 \cdot 10^{-5}\frac{d^{0.5}}{(DT)^{1.5}} \tag{2.65}$$

$$b = 6.359696\frac{d^{0.5}}{(DT)^{0.5}} \tag{2.66}$$

The solvent mixture's density is described by the following formula:

$$d = \sum_s v_s d_s \tag{2.67}$$

In the above expression, v_s is the salt-free volume fraction of the solvent is in the liquid phase and it is computes as follows (*96*):

$$v_s = \frac{x'_s d_s}{\sum_s x'_i d_i} \tag{2.68}$$

Where x'_i is the liquid phase mole fraction of the solvent *i* (salt-free basis), *T* is the temperature, and *D* is the dielectric constant of the solvent mixture. In the case of a binary solvent, the dielectric constant is given by the following expression:

$$D = D_1 + \left[\frac{(D_2 - 1)(2D_2 + 1)}{2D_2} - (D_1 - 1)\right] v_2 \tag{2.69}$$

Where D_1 and D_2 are the pure component dielectric constant of the solvents (*96*). The activity coefficient for the middle range contribution for both solvents and ions is given by:

$$\ln \gamma^{MR}_{solv,k} = \sum_{ion} B_{k,ion} m_{ion} - \frac{M_k \sum_k \sum_i \nu_k^{(i)} x'_i}{M} \sum_k \sum_{ion} \left[B_{k,ion} + IB'_{k,ion}\right] x'_k m_k - \sum_c \sum_a \left[B_{c,a} + IB'_{c,a}\right] m_c m_k \tag{2.70}$$

$$\ln \gamma^{MR}_{solv,} = \sum_k \nu_k^{(i)} \ln \gamma_k^{MR} \tag{2.71}$$

$$\ln \gamma^{MR}_{ion,j} = \frac{1}{M} \sum_{ion} B_{k,ion} x'_k - \frac{z_j^2}{2M} \sum_k \sum_j B'_{k,ion} x'_k + \sum_k B_{c,a} m_c - \frac{z_a^2}{2} \sum_c \sum_a B'_{c,a} m_c m_a \tag{2.72}$$

In the above equations, x'_k is the salt-free mole fraction of solvent group k, $\nu_k^{(i)}$ M_k is the molecular weight of solvent group *k*, *M* is the molecular weight of mixed-solvent. In the LIFAC model, $B_{i,j}$ is a second virial coefficient. This coefficient represents the interaction between the species *i* and *j*. The expressions for the ion-ion interaction parameter $B_{c,a}$ and ion-solvent group interaction parameter $B_{k,ion}$ are given by:

$$B_{c,a} = b_{c,a} + c_{c,a} exp(-I^{0.5} + 0.13I) \quad \textbf{(2.73)}$$

$$B_{k,ion} = b_{k,ion} + c_{k,ion} exp(-1.2I^{0.5} + 0.13I) \quad \textbf{(2.74)}$$

Where $b_{i,j}$ and $c_{i,j}$ are known as the middle range parameters between compound *i* and *j*. These can be either ion or solvents groups and their values are found in the LIFAC tables (*96*). Finally, the complete expression for the activity coefficient of solvent *s* is given by the following expression [*96*]:

$$ln\gamma_s = ln\gamma_s^{LR} + ln\gamma_s^{MR} + ln\gamma_s^{SR} \quad \textbf{(2.75)}$$

Similarly, the activity coefficient for ion *j*, the following equation is presented (*96*):

$$ln\gamma_j = ln\gamma_j^{LR} + ln\gamma_j^{MR} + ln\gamma_j^{SR} - ln\left(\frac{M_s}{M} + M_s \sum_i^{ion} m_i\right) \quad \textbf{(2.76)}$$

In the above equation, m_i is the molality of the *i* ion.

The activity coefficient from the LIFAC model is incorporated into the PSRK expression for the partial fugacity coefficient in PSRK EoS for compound *i* in the mixture as follows:

$$ln\varphi_i = \frac{b_i}{b}(z-1) - ln\left(\frac{P(v-b)}{RT}\right) - \bar{\alpha}_i ln\left(\frac{v+b}{v}\right) \quad \textbf{(2.77)}$$

$$\bar{\alpha}_i = \frac{1}{A_1}\left(\sum_i x_i ln\gamma_i + \sum_i x_i ln\left(\frac{b}{b_i}\right)\right) + \sum_i x_i \frac{a_i}{b_i RT} \quad \textbf{(2.78)}$$

Where *z* is the compressibility factor. In extending the model of Garcia et al. (*23*) to TBAB semi-clathrates formed in the presence of gas mixtures, the mixture is accounted for in the free energy mixing rules, the activity coefficient model as well as the solid phase model. What should be noted is that this approach does not introduce any parameters beyond the available binary interaction parameters.

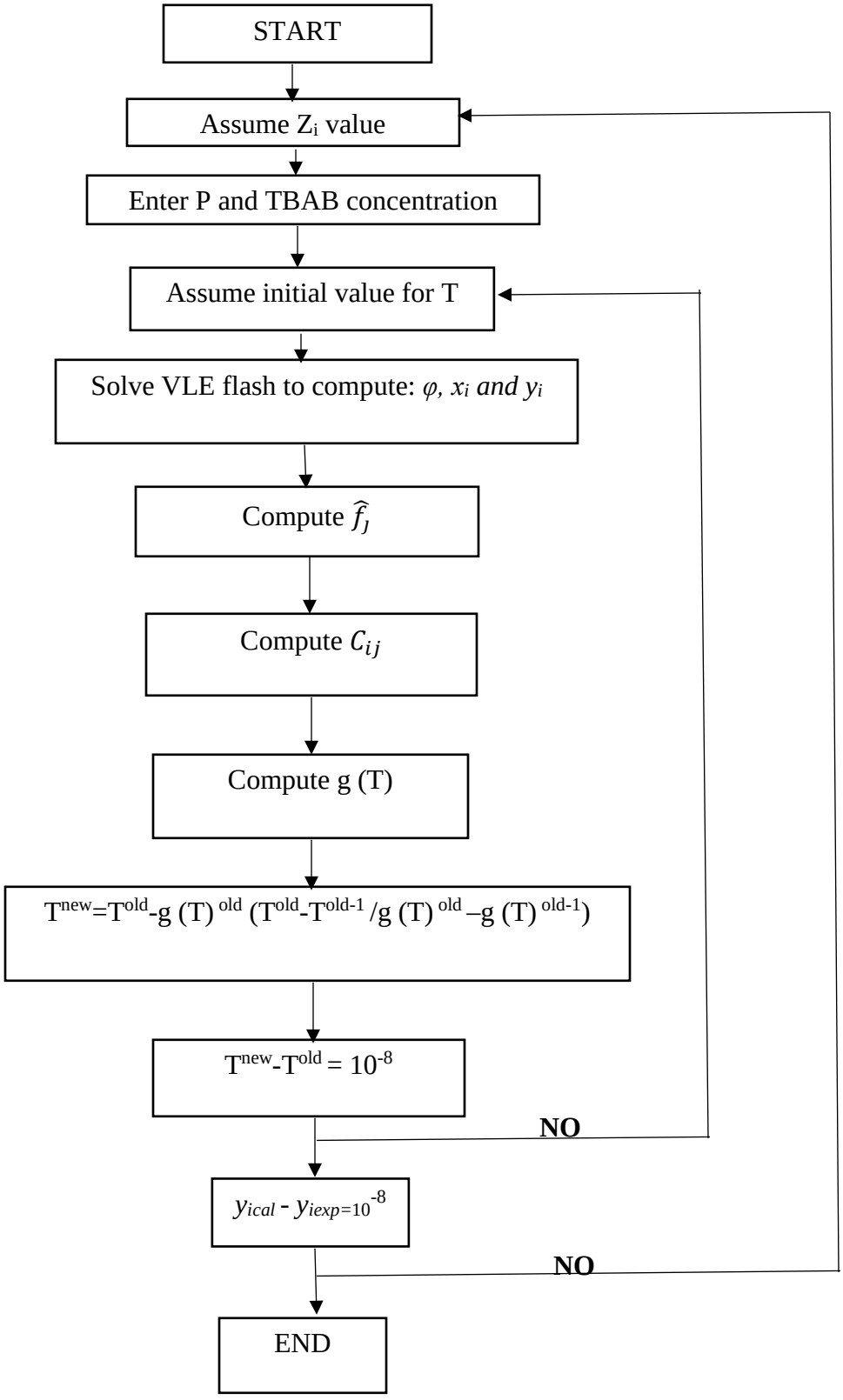

Figure 2.1: Flow diagram for computing the dissociation temperature of semi-clathrates at a given pressure.

The algorithm for solving the three-phase equilibrium is presented in figure 2.1. In order to compute the dissociation temperature using the algorithm, the feed composition of the mixture (z_i), pressure (P), and TBAB concentration must be specified, to satisfy Gibbs Phase Rule. The y_{iexp} mentioned in the algorithm is the experimental vapour phase mole fraction that is obtained from experimental data (*31, 52, and 58*). The y_{ical} is the vapour phase mole fraction that is calculated from the model. The feed composition value ($\boldsymbol{z_i}$) for the entire system at each data point (pressure and temperature) is obtained when the conditions ($y_{ical} - y_{iexp=10^{-8}}$) are satisfied. When solved by secant method (*103, P.10*), the equation (2.34) is expressed as an implicit function of temperature g(T). The feed composition value ($\boldsymbol{z_i}$) computed in the present work are presented in the next session 3.3 of the next chapter. In the present study, the model is developed to predict the dissociation temperature of the semi-clathrate at a given system composition and pressure.

Chapter three: **Results and Discussion**

The thermodynamic model that was presented in the previous chapter has been used to correlate the three-phase equilibrium conditions for binary and ternary mixtures of CO, CO_2, CH_4, H_2 and N_2 (*31, 52, 58*). As noted in the literature review, in addition to the data sets, there are additional data sets for the thermodynamic equilibrium conditions of TBAB semi-clathrates formed in the presence of gas mixtures (*30,38,42,43,45,47,50,53,54,57,59,63*). However, these data sets do not present measurements of y_i and thus, they will not be included in the testing of the model.

3.1 Parameter regression

As previously noted, the model of Garcia et al. (*23*) requires the regression of two adjustable parameters for each semi-clathrate structure and an additional three adjustable parameters for each gas. For the algorithm presented in the previous section, the parameters regressed by Garcia et al. (*23*) will be used where available. Garcia et al. (*23*) regressed structural parameters for TBAB semi-clathrates as well as Kihara potential parameters for pure CO_2, CH_4, H_2 and N_2; these parameters are shown in Table 2.2 and Table 2.3. The only gas whose Kihara potential parameters are not available is CO. In the current study, Kihara potential parameters for CO will be regressed from equilibrium data involving TBAB semi-clathrates formed in the presence of CO-CO_2 mixtures (*31*). Subsequently, the regressed parameters for CO will be tested for its ability to correlate equilibrium data for TBAB semi-clathrates formed in the presence of H_2-CO-CO_2 mixtures (*31*).

To regress the Kihara Potential Parameters for CO, the algorithm from the previous chapter is combined with one of Matlab's built-in parameter optimization algorithms. Specifically, the Nelder-Mead algorithm (*102*) was chosen due to it not requiring analytical expressions for the first derivatives of the objective function. The objective function that was minimized represents the sum of the square of the errors between the measured and the predicted value of the three-phase equilibrium temperature. The objective function is shown below:

$$F = \sum_{i}^{NP} (T^{calc} - T^{exp})^2 \qquad \textbf{(3.1)}$$

Where *F* is the objective function, *NP* is denoted as the number of experimental points, and T^{exp} and T^{cal} are the experimental and calculated temperature of the mixture. The optimized parameters are listed in tables 3.1 and 3.2 The results from the parameter optimization are shown in table 2-4. The standard errors associated with the parameters were computed using the methodology developed by Clarke et al (*97*) (described in Appendix C). As seen in table 2-4, the standard errors are at least one order of magnitude smaller than the computed parameter values. Figure 3.1 shows the associated correlation of the three-phase equilibrium conditions. From figure 3.1 the results are seen to be in excellent agreement with the measured data. This indicates that the parameters are statistically significant. The values obtained in this section will subsequently be used to predict the equilibrium conditions of TBAB semi-clathrates formed in the presence of a ternary mixture of $CO/CO_2/H_2$.

Table 3.1: Semi-clathrate parameters to compute solid-liquid equilibria of the systems H_2O+TBAB and, at atmospheric pressure (Reproduced from Garcia (*22*))

Salt	Type	$\Delta_{dis}H^0(T_0)$/ kJ/mol	$\Delta_{dis}V^0(T)$/ cm^3/mol	AARD %
TBAB	A	155.35 ± 1.52	-5.36 ± 0.045	0.09
TBAB	B	162.56 ± 1.36	-12.15 ± 0.074	0.35

Table 3.2: Regressed Kihara potential parameters for CH_4, CO_2, CO, H_2, and N_2, in TBAB aqueous solutions. Reproduced from Garcia (*22*)

Gas	a (Å)	σ (Å)	ε/k (K)
CH_4	0.41521 ± 0.023	2.95856 ± 4.410^{-4}	$304.25 \pm 6.3*10^{-3}$
CO_2	0.71086 ± 0.015	3.05256 ± 5.610^{-3}	$242.156 \pm 4.8*10^{-2}$
H_2	0.29656 ± 0.036	$3.56415 \pm 6.5*10^{-3}$	$160.75 \pm 3.45*10^{-3}$
N_2	0.37856 ± 0.047	$3.9574 \pm 4.1*10^{-2}$	$174.236 \pm 7.45*10^{-3}$

Table 3.3: Regressed Kihara potential parameters for CO, obtained in the current study.

Gas	a (Å)	σ (Å)	ε/k (K)
CO	0.3677 ± 0.026	$2.9916 \pm 3.1*10^{-2}$	$177.21 \pm 5.70*10^{-2}$

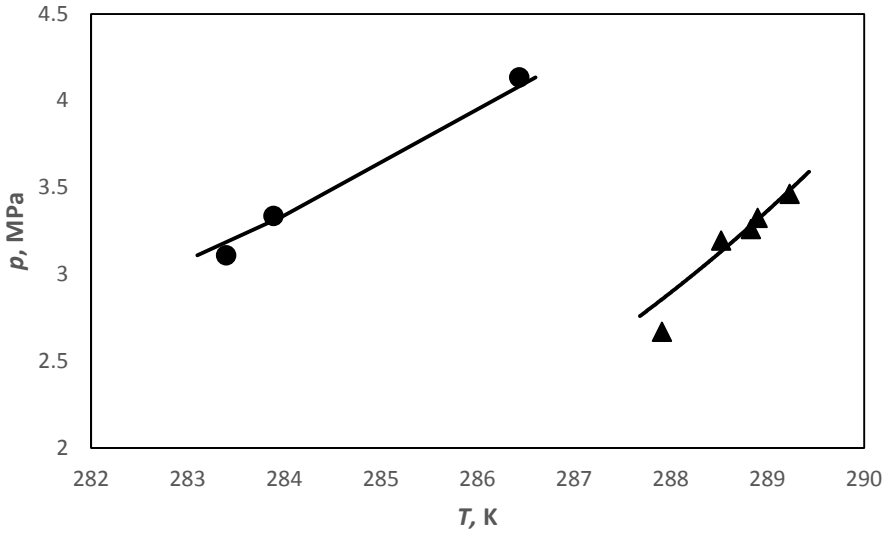

Figure 3.1: Dissociation conditions of semi-clathrate hydrates for the carbon dioxide+carbon monoxide+water/TBAB aqueous solution (*31*) for cylinder composition (CO_2-0.50/CO-0.50). Symbols stand for experimental data and lines refer to the predicted values using the developed thermodynamic model; ●, CO_2+CO in presence of 5 wt% TBAB; ▲, CO_2+CO in presence of 20 wt% TBAB.

The below table 3.4 and 3.5 presents the regressed feed composition values of semi-clathrate formed from the gas mixtures of (CO_2, CO) in the presence of TBAB.

Table 3.4 Feed composition of semi-clathrates of (CO_2+CO) gas mixture for w_{TBAB}=0.05

Components	**Z value for Data Point 1 (286.43/K), (4.135/MPa)**	**Z value for Data point 2 (283.89/K), (3.336/MPa)**	**Z value for Data point 3 (283.4/K), (3.11/MPa)**
CO_2	0.18	0.18	0.18
H_2O	0.63	0.63	0.63
TBAB	$1.93x10^{-3}$	$1.94x10^{-3}$	$1.94x10^{-3}$
CO	0.18	0.18	0.18

Table 3.5 Feed composition of semi-clathrates of (CO_2+CO) gas mixture for w_{TBAB}=0.20

Components	**Z value for Data point 1 (289.23/K), (3.464/MPa)**	**Z value for Data point 2 (288.83/K), (3.261/MPa)**	**Z value for Data point 3 (288.9/K), (3.326/MPa)**	**Z value for Data point 4 (288.52/K), (3.194/MPa)**	**Z value for Data point 5 (287.91/K), (2.67/MPa)**
CO2	0.23	0.23	0.23	0.23	0.23
H2O	0.54	0.54	0.54	0.54	0.54
TBAB	$7.73x10^{-3}$	$7.74x10^{-3}$	$7.73x10^{-3}$	$7.74x10^{-3}$	$7.75x10^{-3}$
CO	0.23	0.23	0.23	0.23	0.23

3.2 Results and discussion

In the present work, several systems that form semi-clathrates of TBAB have been selected to prove the accuracy of the thermodynamic model that is used in the present study. The model is used to correlate the dissociation temperature of the semi-clathrate formed from the gas mixtures

of CO_2, CO, CH_4, N_2, and H_2 (*31*, *52*, *58)*. These data sets are used because they present the measurement of the *yi* values that are required to test the model. The modelling is carried using the algorithm that is outlined in the Chapter 2.

The below figure 3.2 shows the equilibrium condition that was correlated for the semi-clathrates formed from the gas mixtures of (CO_2/N_2) without regressing the feed composition values. From figure 3.2 it can be seen that there is a lot of deviation between the experimental and the predicted values. On an average the AARD% is reported as 15.6% which is considered relatively high. In order to reduce the deviation between the experimental and the predicted value it was necessary to regress the feed composition values. The figure 3.3 in the next session presents the equilibrium condition of the same semi-clathrate system (CO_2+N_2) which has been developed by regressing the feed composition values. On an average the AARD% reported for the system is 3.7%, which is relatively a better prediction when compared to the equilibrium condition that were correlated with out regressing the feed composition values.

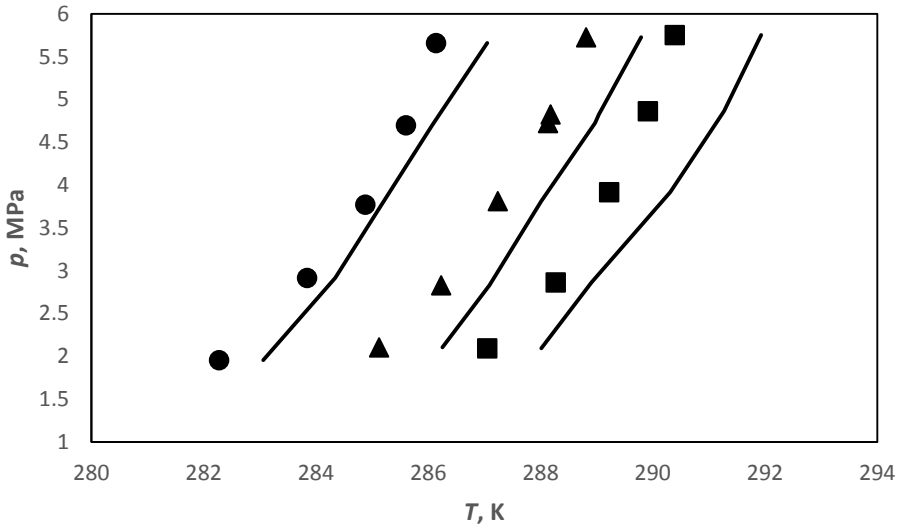

Figure 3.2: Dissociation conditions of semi-clathrate hydrates for the carbon dioxide+nitrogen+water/TBAB aqueous solution systems in the presence of 5 wt.%, 10 wt.% and 20 wt.% of TBAB (*52*) for cylinder composition (CO_2-0.50/N_2-0.50). Symbols stand for experimental data and lines refer to the predicted values using the developed thermodynamic model; ●, CO_2+N_2 in presence of 5 wt% TBAB; ▲, CO_2+N_2 in presence of 10 wt% TBAB; ■, CO_2+N_2 in presence of 20 wt% TBAB.

3.2.1 Semi-clathrates of carbon dioxide and nitrogen gas mixture (CO_2-0.50/N_2-0.50)

The algorithm described in chapter 2 was used to correlate three-phase equlibrium data for TBAB semi-clathrate formed from a gas mixture of carbon dioxide and nitrogen. The model was used to predict the dissociation temprature of the semi-clathrate system of (CO_2+N_2+TBAB) for a cylinder composition of (CO_2-0.50/N_2-0.50) and for different levels of concentration of TBAB (w_{TBAB}=0.05, 0.10, 0.20).

As seen in Figure 3.3, the results of the simulation are in reasonable agreement with the experimental data obtained from Meysel et al (*52*). The regressed feed compositions are presented in Tables 3.6 through 3.8. The present model predicts an AARD value of (**3.6% for w_{TBAB}=0.05), (3.7% for w_{TBAB}=0.10) and (3.8% for w_{TBAB}=0.20)**.

Table 3.6 Feed composition of semi-clathrates of (CO_2+N_2) gas mixture for w_{TBAB}=0.05

Components	**Z value for Data point 1 (282.27/K), (1.956/MPa)**	**Z value for Data point 2 (283.84/K), (2.916/MPa)**	**Z value for Data point 3 (284.88/K), (3.772/MPa)**	**Z value for Data point 4 (285.6/K), (4.699/MPa)**	**Z value for Data point 5 (286.14/K), (5.661/MPa)**
CO_2	0.18	0.18	0.18	0.18	0.18
H_2O	0.63	0.63	0.63	0.63	0.63
TBAB	$1.93x10^{-3}$	$1.92x10^{-3}$	$1.92x10^{-3}$	$1.92x10^{-3}$	$1.91x10^{-3}$
H_2	0.18	0.18	0.18	0.18	0.18

Table 3.7 Feed composition of semi-clathrates of (CO_2+N_2) gas mixture for w_{TBAB}=0.10

Components	Z value for Data point 1 (285.12/K), (2.108/MPa)	Z value for Data point 2 (286.23/K), (2.831/MPa)	Z value for Data point 3 (287.24/K), (3.816/MPa)	Z value for Data point 4 (288.13/K), (4.727/MPa)	Z value for Data point 5 (288.18/K), (4.826/MPa)	Z value for Data point 6 (288.81/K), (5.728/MPa)
CO_2	0.19	0.19	0.19	0.20	0.20	0.20
H_2O	0.60	0.60	0.60	0.60	0.60	0.60
TBAB	$3.86x10^{-3}$	$3.86x10^{-3}$	$3.84x10^{-3}$	$3.83x10^{-3}$	$3.83x10^{-3}$	$3.82x10^{-3}$
H_2	0.19	0.19	0.19	0.20	0.20	0.20

Table 3.8 Feed composition of semi-clathrates of (CO_2+N_2) gas mixture for w_{TBAB}=0.20

Components	Z value for Data Point 1 (287.05/K), (2.095/MPa)	Z value for Data point 2 (288.27/K), (2.865/MPa)	Z value for Data point 3 (289.22/K), (3.920/MPa)	Z value for Data point 4 (289.91/K), (4.866/MPa)	Z value for Data point 5 (290.39/K), (5.754/MPa)
CO_2	0.23	0.23	0.23	0.23	0.23
H_2O	0.53	0.53	0.53	0.53	0.53
TBAB	0.01	0.01	0.01	0.01	0.01
H_2	0.23	0.23	0.23	0.23	0.23

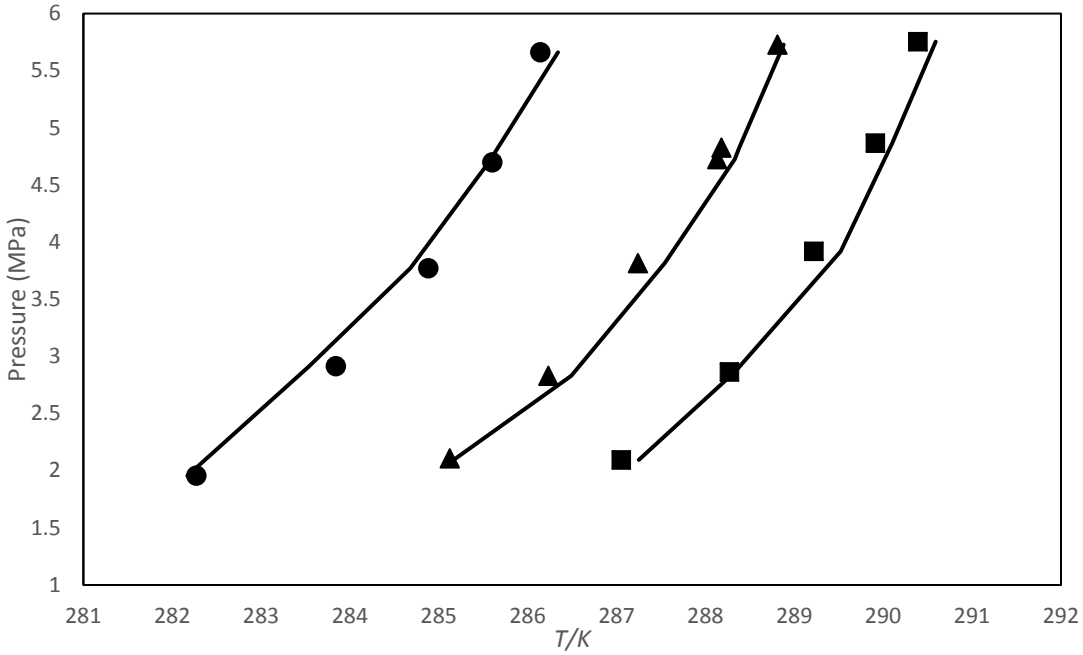

Figure 3.3: Dissociation conditions of semi-clathrate hydrates for the carbon dioxide+nitrogen+water/TBAB aqueous solution systems in the presence of 5 wt.%, 10 wt.% and 20 wt.% of TBAB (*52*) for cylinder composition (CO_2-0.50/N_2-0.50). Symbols stand for experimental data and lines refer to the predicted values using the developed thermodynamic model; ●, CO_2+N_2 in presence of 5 wt% TBAB; ▲, CO_2+N_2 in presence of 10 wt% TBAB; ■, CO_2+N_2 in presence of 20 wt% TBAB.

3.2.2 Semi-clathrates of carbon dioxide and nitrogen gas mixture (CO_2-0.20/N_2-0.80)

The algorithm described in chapter 2 was used to correlate three-phase equlibrium data for TBAB semi-clathrate formed from a gas mixture of carbon dioxide and nitrogen. The model was used to predict the dissociation temperature of the semi-clathrate system of (CO_2+N_2+TBAB) for a cylinder composition of (CO_2-0.20/N_2-0.80) and for different levels of concentration of TBAB (w_{TBAB}=0.05, 0.10, 0.20).

As seen in Figure 3.4, the results of the simulation are in reasonable agreement with the experimental data obtained from Meysel et al (*52*). The regressed feed compositions are presented

in Tables 3.9 through 3.11. The present model predicts an AARD value of (**3.3% for w_{TBAB}=0.05), (3.7% for w_{TBAB}=0.10) and (3.6% for w_{TBAB}=0.20)**.

Table 3.9 Feed composition of semi-clathrates of (CO_2+N_2) gas mixture for w_{TBAB}=0.05

Components	**Z value for Data point 1 (281.75/K), (3.000/MPa)**	**Z value for Data point 2 (283.15/K), (3.870/MPa)**	**Z value for Data point 3 (283.63/K), (4.834/MPa)**	**Z value for Data point 4 (284.43/K), (5.800/MPa)**
CO_2	0.07	0.07	0.07	0.07
H_2O	0.63	0.63	0.63	0.63
TBAB	$1.93*10^{-3}$	$1.93*10^{-3}$	$1.92*10^{-3}$	$1.92*10^{-3}$
N_2	0.29	0.29	0.29	0.29

Table 3.10 Feed composition of semi-clathrates of (CO_2+N_2) gas mixture for w_{TBAB}=0.10

Components	**Z value for Data point 1 (284.57/K), (2.995/MPa)**	**Z value for Data point 2 (285.54/K), (3.915/MPa)**	**Z value for Data point 3 (286.28/K), (4.975/MPa)**	**Z value for Data point 4 (286.99/K), (5.851/MPa)**
CO_2	0.07	0.07	0.07	0.07
H_2O	0.63	0.63	0.63	0.63
TBAB	$4.07*10^{-3}$	$4.06*10^{-3}$	$4.05*10^{-3}$	$4.05*10^{-3}$
N_2	0.29	0.29	0.29	0.29

Table 3.11 Feed composition of semi-clathrates of (CO_2+N_2) gas mixture for w_{TBAB}=0.20

Components	**Z value for Data point 1 (285.72/K), (1.964/MPa)**	**Z value for Data point 2 (286.83/K), (2.523/MPa)**	**Z value for Data point 3 (287.53/K), (3.055/MPa)**	**Z value for Data point 4 (288.28/K), (3.742/MPa)**
CO_2	0.09	0.09	0.09	0.09
H_2O	0.53	0.53	0.53	0.53
TBAB	0.01	0.01	0.01	0.01
N_2	0.37	0.37	0.37	0.37

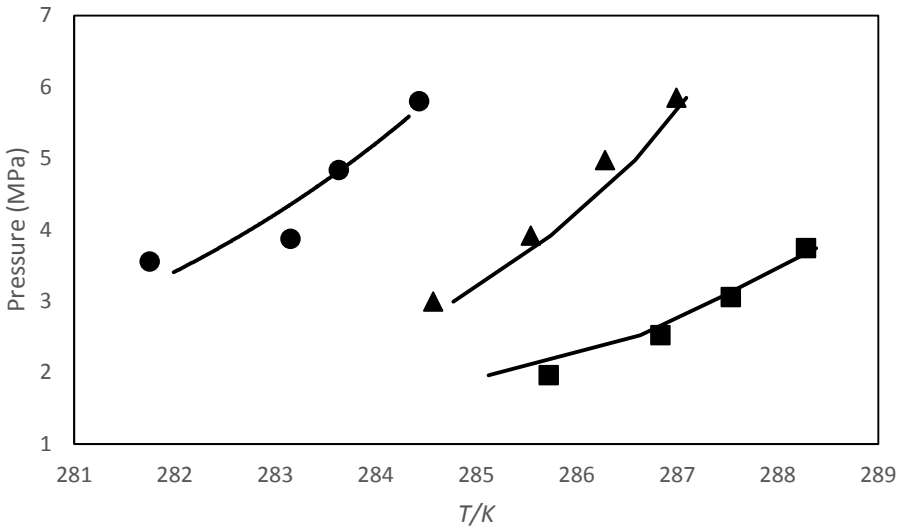

Figure 3.4: Dissociation conditions of clathrate/semi-clathrate hydrates for the carbon dioxide+nitrogen+water/TBAB aqueous solution (*52*) for cylinder composition (CO_2-0.20/N_2-0.80). Symbols stand for experimental data and lines refer to the predicted values using the developed thermodynamic model; ●, CO_2+N_2 in presence of 5 wt% TBAB; ▲, CO_2+N_2 in presence of 10 wt% TBAB; ■, CO_2+N_2 in presence of 20 wt% TBAB.

3.2.3 Semi-clathrates of carbon dioxide and hydrogen gas mixture ($C0_2$-0.40/H_2-0.60)

The algorithm described in chapter 2 was used to correlate three-phase equilibrium data for TBAB semi-clathrates formed from a gas mixture of carbon dioxide and hydrogen. The model was used to predict the dissociation temperature of the semi-clathrate system of (CO_2+H_2+TBAB) for a cylinder composition of (CO_2-0.40/H_2-0.60) and for different levels of concentration of TBAB (w_{TBAB}=0.05, 0.10, 0.20).

As seen in Figure 3.5, the results of the simulation are in reasonable agreement with the experimental data obtained from Wang et al (*31*). The regressed feed compositions are presented in Tables 3.12 through 3.14. It should be noted that, on a water-free basis, the equilibrium gas phase composition is quite different from the cylinder gas-phase composition. This is expected because CO_2 is relatively soluble in water and thus, a non-negligible amount of CO_2 will be absorbed into the liquid solution, by the time equilibrium is achieved. The present model predicts an AARD value of **(5.5% for w_{TBAB}=0.05), (5.7% for w_{TBAB}=0.10) and (5.9% for w_{TBAB}=0.20)**. The values predicted by the present model are better than the predictions of models such as Paricaud's (*90*) in which the AARD values were reported as 10.5%.

Table 3.12 Feed composition of semi-clathrates of (CO_2+H_2) gas mixture for w_{TBAB}=0.05

Components	**Z value for Data point 1 (283.19/K), (4.747/MPa)**	**Z value for Data point 2 (284.51/K), (5.682/MPa)**	**Z value for Data point 3 (284.89/K), (6.189/MPa)**
CO_2	0.14	0.14	0.14
H_2O	0.64	0.64	0.64
TBAB	$1.93*10^{-3}$	$1.93*10^{-3}$	$1.93*10^{-3}$
H_2	0.22	0.22	0.22

Table 3.13 Feed composition of semi-clathrates of (CO_2+H_2) gas mixture for w_{TBAB}=0.10

Components	**Z value for Data point 1 (285.81/K), (4.067/MPa)**	**Z value for Data point 2 (286.53/K), (5.111/MPa)**	**Z value for Data point 3 (287.11/K), (6.326/MPa)**
CO_2	0.16	0.16	0.16
H_2O	0.60	0.60	0.60
TBAB	$3.86*10^{-3}$	$3.86*10^{-3}$	$3.86*10^{-3}$
H_2	0.24	0.24	0.24

Table 3.14 Feed composition of semi-clathrates of (CO_2+H_2) gas mixture for w_{TBAB}=0.20

Components	**Z value for Data point 1 (287.11/K), (3.351/MPa)**	**Z value for Data point 2 (288.24/K), (4.698/MPa)**	**Z value for Data point 3 (289.14/K), (6.245/MPa)**
CO_2	0.18	0.18	0.18
H_2O	0.54	0.54	0.54
TBAB	0.01	0.01	0.01
H_2	0.27	0.27	0.27

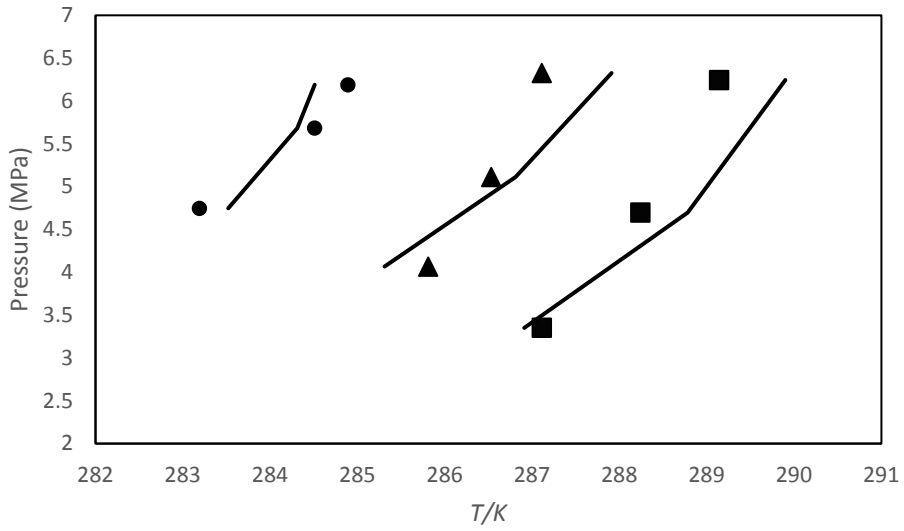

Figure 3.5: Dissociation conditions of semi-clathrate hydrates for the carbon dioxide+hydrogen+water/TBAB aqueous solution (*31*) for cylinder composition (CO_2-0.40/H_2-0.60). Symbols stand for experimental data and lines refer to the predicted values using the developed thermodynamic model; ●, CO_2+H_2 in presence of 5 wt% TBAB; ▲, CO_2+H_2 in presence of 10 wt% TBAB; ■, CO_2+H_2 in presence of 20 wt% TBAB.

3.2.4 Semi-clathrates of carbon dioxide and hydrogen gas mixture ($C0_2$-0.60/H_2-0.40)

The algorithm developed in the present study was used to correlate three-phase equlibrium data for TBAB semi-clathrate formed from a gas mixture of carbon dioxide and hydrogen. The model was used to predict the dissociation temprature of the semi-clathrate system of (CO_2+H_2+TBAB) for a cylinder composition of (CO_2-0.60/H_2-0.40) and for different levels of concentration of TBAB (w_{TBAB}=0.05, 0.10, 0.20).

As seen in Figure 3.4, the results of the simulation are in reasonable agreement with the experimental data obtained from Wang et al (*31*). The regressed feed composition is presented in Table 3.15 through 3.17. In the Figure 3.6, the model predicts an AARD value of **(5.1% for w_{TBAB}=0.05), (5.4% for w_{TBAB}=0.10) and (5.7% for w_{TBAB}=0.20)**.

Table 3.15 Feed composition of semi-clathrates of (CO_2+H_2) gas mixture for w_{TBAB}=0.05

Components	**Z value for Data point 1 (282.50/K), (3.555/MPa)**	**Z value for Data point 2 (284.12/K), (4.324/MPa)**	**Z value for Data point 3 (285.19/K), (6.127/MPa)**
CO_2	0.22	0.22	0.22
H_2O	0.63	0.63	0.63
TBAB	$1.93*10^{-3}$	$1.93*10^{-3}$	$1.93*10^{-3}$
H_2	0.15	0.15	0.15

Table 3.16 Feed composition of semi-clathrates of (CO_2+H_2) gas mixture for w_{TBAB}=0.10

Components	**Z value for Data point 1 (286.85/K), (3.496/MPa)**	**Z value for Data point 2 (287.81/K), (4.693/MPa)**	**Z value for Data point 3 (288.91/K), (6.327/MPa)**
CO_2	0.24	0.24	0.24
H_2O	0.60	0.60	0.60
TBAB	$3.85*10^{-3}$	$3.84*10^{-3}$	$3.80*10^{-3}$
H_2	0.16	0.16	0.16

Table 3.17 Feed composition of semi-clathrates of (CO_2+H_2) gas mixture for w_{TBAB}=0.20

Components	**Z value for Data point 1 (288.89/K), (3.646/MPa)**	**Z value for Data point 2 (289.84/K), (4.808/MPa)**	**Z value for Data point 3 (291.08/K), (6.612/MPa)**
CO_2	0.27	0.28	0.28
H_2O	0.55	0.53	0.53
TBAB	0.01	0.01	0.01
H_2	0.18	0.18	0.18

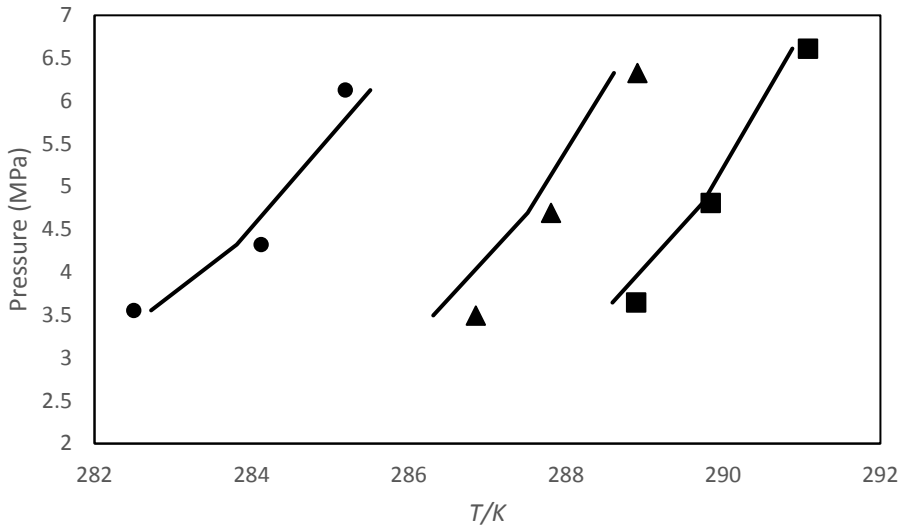

Figure 3.6: Dissociation conditions of semi-clathrate hydrates for the carbon dioxide+hydrogen+water/TBAB aqueous solution (*31*) for cylinder composition (CO_2-0.60/H_2-0.40). Symbols stand for experimental data and lines refer to the predicted values using the developed thermodynamic model; ●, CO_2+H_2 in presence of 5 wt% TBAB; ▲, CO_2+H_2 in presence of 10 wt% TBAB; ■, CO_2+H_2 in presence of 20 wt% TBAB.

3.2.5 Semi-clathrates of carbon dioxide and methane gas mixture (CO_2-0.40/CH_4-0.60)

The algorithm developed in the present study was used to correlate three-phase equlibrium data for TBAB semi-clathrate formed from a gas mixture of carbon dioxide and methane. The model was used to predict the dissociation temprature of the semi-clathrate system of (CO_2+CH_4+TBAB) for a cylinder composition of (CO_2-0.40/CH_4-0.60) and for different levels of concentration of TBAB (w_{TBAB}=0.05, 0.10, 0.20).

As seen in Figure 3.7, the results of the simulation are in reasonable agreement with the experimental data obtained from Acosta et al (*58*). The regressed feed composition is presented in Table 3.18 through 3.20. In the Figure 3.7, the model predicts an AARD value of **(5.9% for w_{TBAB}=0.05), (6.1% for w_{TBAB}=0.10) and (6.3% for w_{TBAB}=0.20)**.

Table 3.18 Feed composition of semi-clathrates of (CO_2+CH_4) gas mixture for w_{TBAB}=0.05

Components	**Z value for Data Point 1 (288.83/K), (6.325/MPa)**	**Z value for Data point 2 (288.47/K), (5.661/MPa)**	**Z value for Data point 3 (287.93/K), (4.893/MPa)**	**Z value for Data point 4 (287.03/K), (3.752/MPa)**	**Z value for Data point 5 (286.26/K), (3.104/MPa)**
CO_2	0.12	0.12	0.12	0.12	0.12
H_2O	0.69	0.69	0.69	0.69	0.69
TBAB	$2.09*10^{-3}$	$2.09*10^{-3}$	$2.09*10^{-3}$	$2.10*10^{-3}$	$2.09*10^{-3}$
CH_4	0.19	0.19	0.19	0.19	0.19

Table 3.19 Feed composition of semi-clathrates of (CO_2+CH_4) gas mixture for w_{TBAB}=0.10

Components	**Z value for Data point 1 (291.02/K), (6.370/MPa)**	**Z value for Data point 2 (290.64/K), (5.741/MPa)**	**Z value for Data Point 3 (289.64/K), (4.672/MPa)**	**Z value Data point 4 (288.96/K), (3.952/MPa)**	**Z value for Data point 5 (288.14/K), (3.011/MPa)**
CO_2	0.14	0.14	0.14	0.14	0.14
H_2O	0.65	0.65	0.65	0.65	0.65
TBAB	$4.20*10^{-3}$	$4.20*10^{-3}$	$4.21*10^{-3}$	$4.22*10^{-3}$	$4.16*10^{-3}$
CH_4	0.21	0.21	0.21	0.21	0.21

Table 3.20 Feed composition of semi-clathrates of (CO_2+CH_4) gas mixture for w_{TBAB}=0.20

Components	**Z value for Data point 1 (292.59/K), (6.229/MPa)**	**Z value for Data point 2 (291.69/K), (4.846/MPa)**	**Z value for Data point 3 (290.85/K), (3.857/MPa)**	**Z value for Data point 4 (289.84/K), (2.972MPa)**
CO_2	0.17	0.17	0.17	0.17
H_2O	0.58	0.58	0.58	0.58
TBAB	0.01	0.01	0.01	0.01
CH_4	0.25	0.25	0.25	0.25

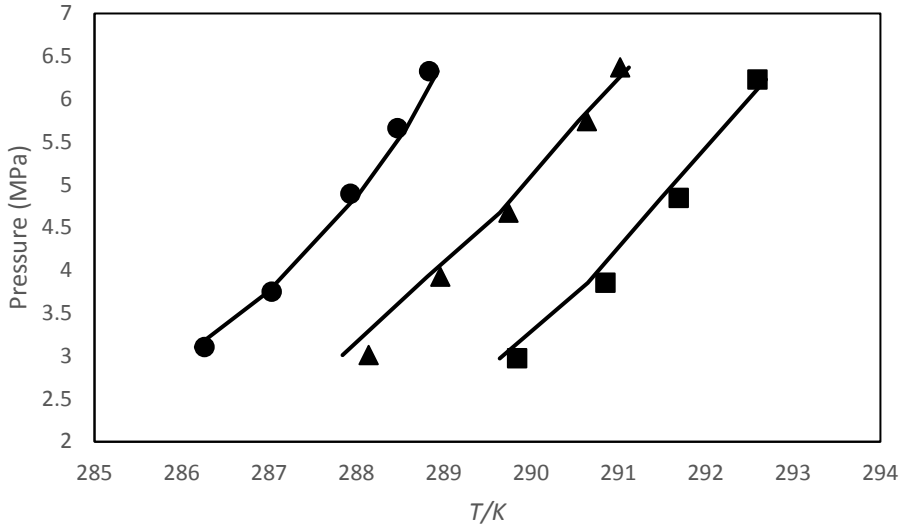

Figure 3.7: Dissociation conditions of clathrate/semi-clathrate hydrates for the carbon dioxide+methane+water/TBAB aqueous solution (*58*) for cylinder composition (CO_2-0.40/CH_4-0.60). Symbols stand for experimental data and lines refer to the predicted values using the developed thermodynamic model; ●, CO_2+CH_4 in presence of 5 wt% TBAB; ▲, CO_2+CH_4 in presence of 10 wt% TBAB; ■, CO_2+CH_4 in presence of 20 wt% TBAB.

3.2.6 Semi-clathrates of carbon dioxide and methane gas mixture (CO_2-0.60/CH_4-0.40)

The algorithm developed in the present study was used to correlate three-phase equlibrium data for TBAB semi-clathrate formed from a gas mixture of carbon dioxide and methane. The

model was used to predict the dissociation temprature of the semi-clathrate system of (CO_2+CH_4+TBAB) for a cylinder composition of (CO_2-0.60/CH_4-0.40) and for different levels of concentration of TBAB (w_{TBAB}=0.05, 0.10, 0.20).

As seen in Figure 3.8, the results of the simulation are in reasonable agreement with the experimental data obtained from Acosta et al (*58*). The regressed feed composition is presented in Table 3.21 through 3.23. In the Figure 3.8, the model predicts an AARD value of **(5.7% for w_{TBAB}=0.05), (5.9% for w_{TBAB}=0.10) and (6.1% for w_{TBAB}=0.20)**.

Table 3.21 Feed composition of semi-clathrates of (CO_2+CH_4) gas mixture for w_{TBAB}=0.05

Components	**Z value for Data Point 1 (289.46/K), (6.493/MPa)**	**Z value for Data point 2 (288.96/K), (5.026/MPa)**	**Z value for Data point 3 (288.44/K), (4.498/MPa)**	**Z value for Data point 4 (287.47/K), (3.669/MPa)**	**Z value for Data point 5 (286.73/K), (2.866/MPa)**
CO_2	0.25	0.25	0.25	0.25	0.25
H_2O	0.58	0.58	0.58	0.58	0.59
TBAB	$1.78*10^{-3}$	$1.79*10^{-3}$	$1.79*10^{-3}$	$1.79*10^{-3}$	$1.80*10^{-3}$
CH_4	0.17	0.17	0.17	0.17	0.17

Table 3.22 Feed composition of semi-clathrates of (CO_2+CH_4) gas mixture for w_{TBAB}=0.10

Components	**Z value for Data point 1 (291.41/K), (6.54/MPa)**	**Z value for Data point 2 (290.47/K), (4.974/MPa)**	**Z value for Data point 3 (289.36/K), (3.775/MPa)**	**Z value for Data point 4 (288.51/K), (2.828/MPa)**
CO_2	0.21	0.21	0.21	0.21
H_2O	0.65	0.65	0.65	0.65
TBAB	$4.19*10^{-3}$	$4.21*10^{-3}$	$4.23*10^{-3}$	$4.24*10^{-3}$
CH_4	0.14	0.14	0.14	0.14

Table 3.23 Feed composition of semi-clathrates of (CO_2+CH_4) gas mixture for w_{TBAB}=0.20

Components	Z value for Data point 1 (293.00/K), (6.407/MPa)	Z value for Data point 2 (292.51/K), (5.471/MPa)	Z value for Data point 3 (292.02/K), (4.477/MPa)	Z value for Data point 4 (291.32/K), (3.626/MPa)	Z value for Data point 5 (290.39/K), (2.972/MPa)
CO_2	0.25	0.25	0.25	0.25	0.25
H_2O	0.58	0.58	0.58	0.58	0.58
TBAB	0.01	0.01	0.01	0.01	0.01
CH_4	0.17	0.17	0.17	0.17	0.17

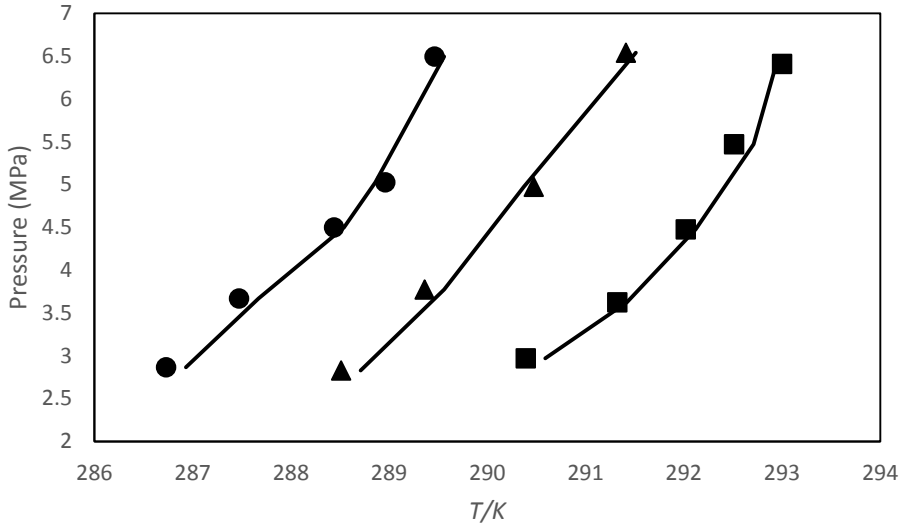

Figure 3.8: Dissociation conditions of clathrate/semi-clathrate hydrates for the carbon dioxide+methane+water/TBAB aqueous solution (*58*) for cylinder composition (CO_2-0.60/CH_4-0.40). Symbols stand for experimental data and lines refer to the predicted values using the developed thermodynamic model; ●, CO_2+CH_4 in presence of 5 wt% TBAB; ▲, CO_2+CH_4 in presence of 10 wt% TBAB; ■, CO_2+CH_4 in presence of 20 wt% TBAB.

3.2.7 Semi-clathrates of carbon dioxide, carbon monoxide, and hydrogen gas mixture

The algorithm developed in the present study was used to correlate three-phase equlibrium data for TBAB semi-clathrate formed from a gas mixture of carbon dioxide, carbon monoxide and hydrogen. The model was used to predict the dissociation temprature of the semi-clathrate system of (CO_2+CO_2+H_2+TBAB) for a cylinder composition of (CO_2-0.0991/CO-0.6059/H_2-0.295).

As seen in Figure 3.9, the results of the simulation are in reasonable agreement with the experimental data obtained from Wang et al (*31*). The regressed feed composition is presented in Table 3.24. For the ternary mixture model predicts an AARD% value of 7.1% for $\boldsymbol{w_{TBAB}}$**=0.20**.

Table 3.24 Feed composition of semi-clathrates of (CO_2+CO+H_2) gas mixture for w_{TBAB}=0.20

Components	**Z value for Data point 1 (286.75/K), (4.396/MPa)**	**Z value for Data point 2 (286.44/K), (3.993/MPa)**	**Z value for Data point 3 (285.84/K), (3.317/MPa)**	**Z value for Data point 4 (285.44/K), (2.837/MPa)**
TBAB	0.01	0.01	0.01	0.01
CO2	0.05	0.05	0.05	0.05
H2O	0.53	0.53	0.53	0.53
CO	0.27	0.27	0.27	0.27
H2	0.13	0.14	0.14	0.14

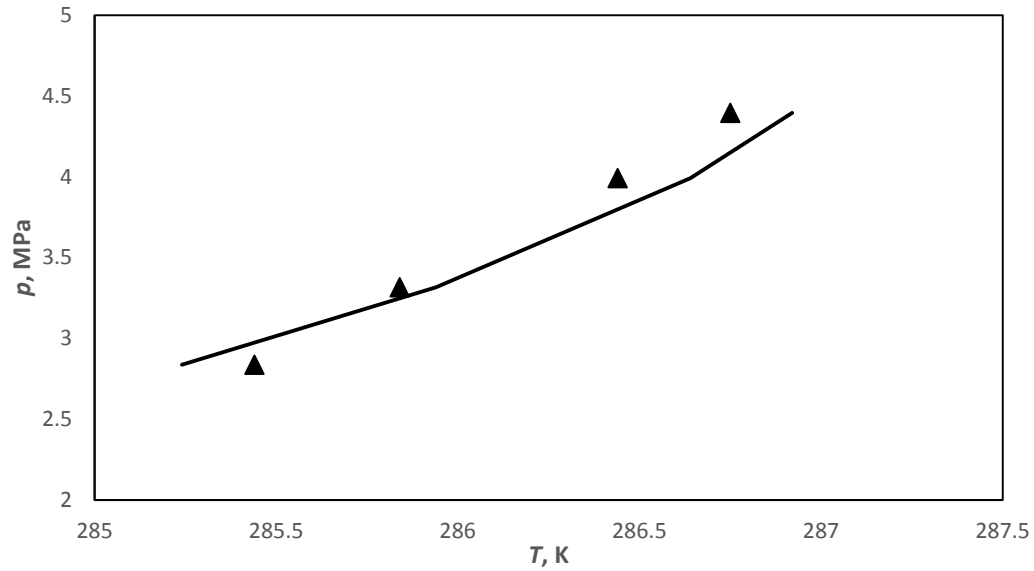

Figure 3.9: Dissociation conditions of semi-clathrate hydrates of (CO_2+CO+H2+H_2O/TBAB) systems (*58*) for cylinder composition (CO_2-0.0991/CO-0.6059/H_2-0.295). Symbols stand for experimental data and lines refer to the predicted values using the developed thermodynamic model; ▲, CO_2+CO+H_2 in presence of 20 wt% TBAB.

Chapter four **Conclusion and recommendation**

4.1 Conclusions

The main aim of this work was to develop a thermodynamic approach to correlate the equilibrium conditions of semi-clathrate formed from the gas mixture of (CO_2, CO, CH_4, H_2 and N_2) in the presence of TBAB. To achieve it, the following steps were undertaken in the present work. First, a brief introduction about gas hydrate and how different they are from semi-clathrate was presented, followed by potential applications of the semi-clathrate like separation of greenhouse gases and their experimental studies were reviewed and discussed in detail. Later, a detailed review of the thermodynamic models that are available in the open literature was presented in detail. From the review, it was inferred that there is a need for developing a reliable thermodynamic model since there are not many models that are available in the open literature that could correlate the equilibrium conditions of the semi-clathrate formed from the gas mixtures.

The thermodynamic approach proposed in the present study is based on the extension of work done by Garcia (*22*). Originally Garcia (*22*), developed a thermodynamic model to correlate the equilibrium conditions of the semi-clathrate formed from pure gases. In the present study, the model developed by Garcia (*22*) is extended to predict the equilibrium and dissociation conditions of the semi-clathrate formed from the gas mixtures, in the presence of TBAB.

The PSRK equation of state is used to describe the fluid and the vapour phase. A flash was performed to determine the composition of all the components in the vapour and liquid phase. The LIFAC model was used to compute the activity coefficients, of the electrolyte species in the fluid phase. The Kihara potential was used to compute the Langmuir constants. The important feature of the extended thermodynamic model is, it could calculate the feed composition values of semi-clathrate formed from the gas mixtures of (CO_2, CO, CH_4, H_2 and N_2) in the presence of TBAB, using the experimental data's that are available in the open literature. Apart from the binary mixture, the model was used to predict the dissociation conditions of the ternary mixture and a % AARD (average relative deviation) value of 7.1% was reported by the model. From the literature review, it was observed that none of the previously developed thermodynamic models predicted the equilibrium conditions of semi-clathrates formed from ternary gas mixtures. The % ARD (average relative deviation) of the calculated and experimental values were in the range of 3.2% to 7.2%.

Except for Paricaud (*90*) when comparing with the models that were previously developed. The current model requires the least number of adjustable parameters (five parameters). The values predicted from the model were in good agreement with the experimental data, when compared with other models the obtained values were considerably superior.

4.2 Recommendations

Based on the present study, the following recommendations are recommended:

- Due to the lack of experimental data on semi-clathrates formed from other promoters like TBAC, $TBANO_3$ and TBPB in the open literature. The current work only focuses on the semi-clathrates formed from the gas mixtures in the presence of TBAB. The future experimental and computational works can be focused on semi-clathrate formed from the above-mentioned promoters.
- From the literature review, it is observed that except for the experimental values published by Wang et al (*31*) there are no experimental data available in the open literature for the semi-clathrate formed from a ternary gas mixture. Hence the future experimental works can be based on measuring the equilibrium conditions of semi-clathrate formed from ternary gas mixtures.

BIBLIOGRAPHY

[1] J. Carroll, Natural Gas Hydrates, A Guide for Engineers, second ed. ed., Burlington, MA: Gulf Professional Publishing, 2009.

[2] H. Davy, "On a Combination of oxymuriatic gas and oxygene gas.," *Phil. Trans. Roy. Soc. Lond.*, vol. 101, pp. 155-162, 1811.

[3] M. Faraday, "On Hydrate of Chlorine," *Quart. J. Sci. Lit. Arts.*, vol. 15, pp. 71-74, 1823.

[4] N. I. Papadimitriou, I. N. Tsimpanogiannis and A. K. Stubos, "Gas Content of Binary Clathrate Hydrates with Promoters," *J. Chem. Phys.* , pp. 0441021-0441027, 2009.

[5] E. D. Sloan and C. A. Koh, Clathrates Hydrates of Natural Gases, New York: CRC Press-Taylor and Francis Group, 2008.

[6] D. A. Avlonitis and N. Varotsis, "Modelling Gas Hydrate Thermodynamics Behaviour: Theoretical Basis and Computational Methods," *Fluid Phase Equilibria,* vol. 123, pp. 107-130, 1996.

[7] E. G. Hammerschmidt, "Formation of Gas Hydrates in Natural Gas Transmission Lines," *Ind. Eng. Chem.,* vol. 26, pp. 851-855, 1934.

[8] W. R. Parrish and J. M. Prausnitz, "Dissociation Pressures of Gas Hydrates Formed by Gas Mixtures," *Ind. Eng. Chem. Process Des Develop.,* vol. 11, no. 1, pp. 26-35, 1972.

[9] C. A. Koh, E. D. Sloan, A. K. Sum and D. T. Wu, "Fundamentals and Applications of Gas Hydrates," *Annu. Rev. Chem. Biomol. Eng.*, vol. 2, pp. 237-257, 2011.

[10] D. L. Fowler, W. V. Loebenstein, D. B. Pall and C. A. Kraus, "Some Unusual Hydrates of Quaternary Ammonium Salts," *JACS,* vol. 62, pp. 1140-1162, 1940.

[11] R. McMullan and G. A. Jeffrey, "Hydrates of the n-butyl and Tetra i-amyl Quaternary Ammonium Salts," *J. Chem. Phys.*, vol. 31, no. 5, pp. 1231-1234, 1959.

[12] G. A. Jeffrey, "Water Structure in Organic Hydrates," *Acc. Chem. Res.*, vol. 2, pp. 344-354, 1969.

[13] T. V. Rodionova, V. Y. Komarov, G. V. Villevand, T. D. Karpova, N. V. Kuratieva and A. Y. Manakov, "Calorimetric and Structural Studies of Tetrabutylammonium Bromide Ionic Clathrate Hydrates," *J. Phys. Chem. B,* vol. 117, pp. 10677-10685, 2013.

[14] W. Shimada, M. Shiro, H. Kondo, H. Takeya, T. Ebinuma and H. Narita, "Tetra-n-butyl ammonium Bromide-water (1/38) prueba," *Cryst. Struct. Commun.,* vol. 61, pp. o65-o66, 2005.

[15] A. Chapoy, R. Anderson and T. Bahman, "Low-Pressure Molecular Hydrogen Storage in Semi-clathrate Hydrates of Quaternary Ammonium Compounds," *J. Am. Chem. Soc.,* vol. 129, pp. 746-747, 2007.

[16] T. Rodionova, V. Komarov, L. Villevald, L. Aladko, T. Karpova and A. Manakov, "Calorimetric and Structural Studies of Tetrabutylammonium Chloride Ionic Clathrate Hydrates," *J. Phys. Chem. B,* vol. 114, pp. 11838-11846, 2010.

[17] W. Shimada, M. Shiro, H. Kondo, H. Takeya, T. Ebinuma and H. Narita, "Tetra-n-butyl ammonium Bromide-water (1/38) prueba," *Cryst. Struct. Commun.,* vol. 61, pp. o65-o66, 2005.

[18] M. R. Walsh, J. D. Rainey, P. G. Lafond, D. H. Park, D. T. Beckham, M. D. Jones, K. H. Lee, C. A. Koh, E. D. Sloan, D. T. Wu and A. K. Sum, "The Cages, Dynamics, and Structuring of Incipient methane Cathrate Hydrates," *Phys. Chem. Chem. Phys,* vol. 13, pp. 19951-19959, 2011.

[19] L. A. Gaponenko, S. F. Solodovnikov, Y. A. Dyadin, L. S. Aladko and T. M. Polyanskaya, "Crystallographic Study of Tetra-n-butyl Ammonium Bromide," *J. Estruct. Chem*, vol. 25, pp. 157-159, 1984.

[20] H. Nakayama, "Soli-Solid and Liquid-Liquid Phase Equilibria in the Symmetrical Tetraalkylammonium Halide-Water Systems," *Chem. Soc. Jpn.,* vol. 54, pp. 3717-3722, 1981.

[21] H. Oyama, W. Shimada, T. Ebunuma, Y. Kamata, S. Takeya, T. Uchida, J. Nagao and H. Narita, "Phase Diagram, Latent Heat, and Specific Heat of TBAB Semiclathrate Hydrate Crystals," *Fluid Phase Equilibria,* vol. 234, pp. 131-135, 2005.

[22] Marlon Garcia, Measuring and Modelling of the Thermodynamic Equilibrium Conditions for the Formation of TBAB and TBAC Semi-Clathrates Formed in presence of Xenon and Argon, M.Sc thesis, Calgary: University of Calgary, 2015.

[23] M. I. Garcia and M. A. Clarke, "Equilibrium Conditions for TBAB and TBAC Semiclathrates of Xenon and Argon," *J. Chem. Eng. Data,* vol. 59, pp. 3785-3790, 2014.

[24] A. Eslamimanesh, A. H. Mohammadi, D. Richon, P. Naidoo and D. Ramjugernath, "Application of gas hydrate formation in sepration processes: A review of experimental studies," *J. Chem. Thermodyn.,* vol. 46, pp. 62-71, 2012.

[25] Z. G. Sun, L. J. Jiao, Z. G. Zhao, G. L. Wang and H. F. Huang, "Phase Equilibrium Conditions of Semi-Calthrate Hydrates of (Tetra-n-Butyl Ammonium Chloride+Carbon Dioxide)," *J. Chem. Thermodynamics,* vol. 75, pp. 116-118, 2014..

[26] M. Ricaurte, C. Dicharry, D. Broseta, X. Renaud and J. P. Torre, "CO2 Removal from a CO2−CH4 Gas Mixture by Clathrate Hydrate Formation Using THF and SDS as Water-Soluble Hydrate Promoters," *Ind. Eng. Chem. Res. ,* vol. 52, pp. 899-910, 2013..

[27] M. M. van den Heuvel, R. Witteman and C. J. Peters, "Phase behaviour of gas hydrates of carbon dioxide in the presence of tetrahydropyran, cyclobutanone,cyclohexane and methylcyclohexane," *Fluid Phase Equilibria,* vol. 182, pp. 97-110, 2001.

[28] Z. G. Sun, L. J. Jiao, Z. G. Zhao, G. L. Wang and H. F. Huang, "Phase Equilibrium Conditions of Semi-Calthrate Hydrates of (Tetra-n-Butyl Ammonium Chloride+Carbon Dioxide)," *J. Chem. Thermodynamics,* vol. 75, pp. 116-118, 2014.

[29] A. Kumar, T. Sakpal, P. Linga and R. Kumar , "Influence of Contact Medium and Surfactants on Carbon Dioxide Clathrate Hydrate," *Fuel,* vol. 105, pp. 664-671, 2013.

[30] J. Deschamps and D. Dalmazzone, "Dissociation Enthalpies and Phase Equilibrium for TBAB Semi-Clathrate Hydrates of N2, CO2, N2 + CO2 and CH4 + CO2," *J.Therm. Anal. Calorim.*, vol. 98, pp. 113-118, 2009.

[31] S. Wang, M. Danner, T. Kuchling and M. A. Clarke, "Measurement of the Three-Phase (Vapour+Liquid+Solid) Equilibrium Conditions of Semi-Clathrates formed from Mixtures of CO2,CO and H2," *J. Chem. Therm.*, vol. 56, pp. 149-152, 2013.

[32] N. Ye and P. Zhang, "Phase equilibrium and morphology Characteristics of Hydrates Formed by Tetra-n-butyl Ammonium Chloride and Tetra-n-butyl Phosphonium Chloride with and without CO2," *Fluid Phase Equilibria* , vol. 361, p. 208–214, 2014.

[33] N. Mayoufi, D. Dalmazzone, A. Delahaye, P. Clain, L. Fournaison and W. Fürst , "Experimental Data on Phase Behavior of Simple Tetrabutylphosphonium Bromide (TBPB) and Mixed CO2+TBPB Semiclathrate Hydrates," *J. Chem. Eng. Data,* vol. 56, p. 2987–2993, 2011.

[34] S. Li, S. Fan, J. Wang, X. Lang and D. Liang, "CO2 capture from binary mixture via forming hydrate with the help of tetra-n-butyl ammonium bromide," *Journal of Natural Gas Chemistry,* vol. 18, pp. 15-20, 2009.

[35] W. Lin, D. Dalmazzone, W. Fürst, A. Delahaye, L. Fournaison and P. Clain, "Thermodynamic properties of semiclathrate hydrates formed from the TBAB + TBPB + water and CO2 + TBAB + TBPB + water systems," *the TBAB + TBPB + water and CO2 + TBAB + TBPB + water systems,* vol. 372, pp. 63-68, 2014.

[36] A. H. Mohammadi, A. Eslamimanesh, V. Belandria and D. Richon, "Phase Equilibria of Semiclathrate Hydrates of CO2, N2, CH4, or H2 + Tetra-n-butylammonium Bromide Aqueous Solution," *J. Chem. Eng. Data 2011, 56, ,* vol. 56, p. 3855–3865, 2011.

[37] W. Lin, A. Delahaye and L. Fournaison, "Phase Equilibrium and Dissociation Enthalpy for Semi-Clathrate Hydrate of CO2+TBAB," *Fluid Phase Equilibria,* vol. 264, pp. 220-227, 2008.

[38] N. H. Duc, F. Chauvy and J. M. Herri, "CO2 capture by hydrate crystallization – A potential solution for gas emission of steelmaking industry," *Energy Conversion and Management,* vol. 48, p. 1313–1322, 2008.

[39] Y. Seo, S. P. Kang, S. Lee and H. Lee, "Experimental Measurements of Hydrate Phase Equilibria for Carbon Dioxide in the Presence of THF, Propylene Oxide, and 1,4-Dioxane," *J. Chem. Eng. Data,* vol. 53, pp. 2833-2837, 2008.

[40] S. P. Kang, H. Lee, C. S. Lee and W. M. Sung, "Hydrate Phase Equilibria of the Guest Mixtures Containing CO2, N2 and Tetrahydrofuran," *Fluid Phase Equilibria,* vol. 185, pp. 101-109, 2001.

[41] N. Mayouf, D. Dalmazzone, W. Furst, A. Delahaye and L. Fournaison, "CO2 Enclathration in Hydrates of Peralkyl-(Ammonium/Phosphonium) Salts: Stability Conditions and Dissociation Enthalpies," *J. Chem. Eng. Data,* vol. 55, pp. 1271-1275, 2010.

[42] V. Belandria, A. H. Mohammadi, A. Eslamimanesh, D. Richon, M. F. Sanchez-Mora and L. A. Galicia-Luna, "Phase equilibrium measurements for semi-clathrate hydrates of the (CO2 + N2 + tetra-n-butylammonium bromide) aqueous solution systems: Part 2," *Fluid Phase Equilibria,* Vols. 322-323, pp. 105-112, 2012.

[43] A. H. Mohammadi, A. Eslamimanesh, V. Belandria, D. Richon, P. Naidoo and D. Ramjugernath, "Phase Equilibrium Measurements for Semi-Clathrate Hydrates of the (CO2 + N2 + tetra-n-butylammonium bromide) Aqueous Solution System," *J. Chem. Thermodyn.,* vol. 46, pp. 57-61, 2012.

[44] S. Li, S. Fan, J. Wang, X. Lang and Y. Wang, "Clathrate Hydrate Capture of CO2 from Simulated Flue Gas with Cyclopentane/Water Emulsion," *Chinese Journal of Chemical Engineering,* vol. 18, no. 2, pp. 202-206, 2010.

[45] X. S. Li, Z. M. Xia, Z. Y. Chen, K. F. Yan, G. Li and H. J. Wu, "Equilibrium Hydrate Formation Conditions for the Mixtures of CO2 + H2 + Tetrabutyl Ammonium Bromide," *J. Chem. Eng. Data,* vol. 55, p. 2180–2184, 2010.

[46] P. Linga, A. Adeyemo and P. Englezos, "Medium-Pressure Clathrate Hydrate/Membrane Hybrid Process for Postcombustion Capture of Carbon Dioxide," *Environ. Sci. Technol.,* vol. 42, pp. 315-320, 2008.

[47] S. S. Fan, G. F. Chen and T. M. Guo, "Experimental and modeling studies on the hydrate formation of CO2 and CO2-rich gas mixtures," *Chem. Eng. J.,* vol. 78, pp. 173-178, 2000.

[48] S. Fan, S. Li, J. Wang, X. Lang and Y. Wang, "Efficient capture of CO2 from simulated flue gas by formation of TBAB or TBAF semiclathrate hydrates," *Energy & Fuels,* vol. 23, pp. 4202-4208, 2009.

[49] S. P. Kang and H. Lee, "Recovery of CO2 from Flue Gas Using Gas Hydrate: Thermodynamic Verification through Phase Equilibrium Measurements," *Environ. Sci. Technol.,* vol. 34, pp. 4397-4400, 2000.

[50] X. S. Li, C. G. Xu, Z. Y. Chen and H. J. Wu, "Tetra-n-butyl Ammonium Bromide Semi-Clathrate Hydrate Process for Post-Combustion Capture of Carbon Dioxide in the Presence of Dodecyl Trimethyl Ammonium Chloride," *Energy,* vol. 35, pp. 3902-3908, 2010.

[51] Q. L. Ma, G. J. Chen, C. F. Ma and L. W. Zhang, "Study of Vapor-Hydrate two-phase Equilibria," *Fluid Phase Equilibria,* vol. 265, pp. 84-93, 2008.

[52] P. Meysel, L. Oellrich, R. P. Bishnoi and M. A. Clarke, "Experimental Investigation of Incipient Equilibrium Conditions for the Formation of Semi-clathrate Hydrates from Quaternary Mixtures of (CO2 + N2 + TBAB + H2O).," *J. Chem. Thermodyn,* vol. 43, pp. 1475-1479, 2011.

[53] S. M. Kim, J. D. Lee, E. K. Lee and Y. Kim, "Gas hydrate formation method to capture the carbon dioxide for pre-combustion process in IGCC plant," *International Journal of Hydrogen Energy,* vol. 36, pp. 1115-1121, 2011.

[54] B. Zhang and Q. Wu, "Thermodynamic Promotion of Tetrahydrofuran on Methane Separation from Low-Concentration Coal Mine Methane Based on Hydrate," *Energy & Fuels,* vol. 24, p. 2530–2535, 2010.

[55] Z. G. Sun and C. G. Liu, "Equilibrium Conditions of Methane in Semiclathrate Hydrates of Tetra-n-butylammonium Chloride," *J. Chem. Eng.Data,* vol. 57, pp. 978-981, 2012.

[56] Z. G. Sun and L. Sun, "Equilibrium Conditions of Semi-Clathrate Hydrate Dissociation for Methane + Tetra-n-butyl Ammonium Bromide," *J. Chem. Eng. Data,* vol. 55, p. 3538–3541, 2010.

[57] Q. Sun, X. Guo, A. Liu, B. Liu, Y. Huo and G. Chen, "Experimental Study on the Separation of CH4 and N2 via Hydrate Formation in TBAB Solution," *Ind. Eng. Chem. Res.,* vol. 50, p. 2284–2288, 2011.

[58] H. Y. Acosta, P. R. Bishnoi and M. A. Clarke, "Experimental Measurements of the Thermodynamic Equilibrium Conditions of Tetra-n-butylammonium Bromide Semiclathrates Formed from Synthetic Landfill Gases," *J. Chem. Eng. Data,* vol. 56, pp. 69-73, 2011.

[59] S. Fan, Q. Li, J. Nie, X. Lang, Y. Wen and Y. Wang, "Semiclathrate Hydrate Phase Equilibrium for CO2/CH4 Gas Mixtures in the Presence of Tetrabutylammonium Halide (Bromide, Chloride,or Fluoride)," | *J. Chem. Eng. Data* , vol. 58, p. 3137−3141, 2013.

[60] B. Zhang and Q. Wu, "Thermodynamic Promotion of Tetrahydrofuran on Methane Separation from Low-Concentration Coal Mine Methane Based on Hydrate," *Energy & Fuels*, vol. 24, p. 2530–2535, 2010.

[61] W. Kondo, H. Ogawa, R. Ohmura and Y. Mori, "Clathrate Hydrate Formation from a Hydrocarbon Gas Mixture:Evolution of Gas-Phase Composition in a Hydrate-Forming Reactor," *Energy & Fuels,* vol. 24, p. 6375–6383, 2010.

[62] Y. S. Sun, G. J. Chen and L. W. Zhang, "Hydrate phase equilibrium and structure for (methane + ethane + tetrahydrofuran + water) system," *J. Chem. Thermodynamics*, vol. 42, p. 1173–1179, 2010.

[63] Q. Ma, G. Chen and L. Zhang, "Vapor-hydrate phases equilibrium of (CH4+C2H6) and (CH4+C2H4) systems," *Pet. Sci.*, vol. 5, pp. 359-366, 2008.

[64] S. Hashimoto, T. Sugahara, M. Moritoki, H. Sato and K. Ohgaki, "Thermodynamic stability of hydrogen + tetra-n-butyl ammonium bromide mixed gas hydrate in nonstoichiometric aqueous solutions," *Chemical Engineering Science*, vol. 63, pp. 1092-1097, 2008.

[65] Y. Fujisawa, T. Tsuda, S. Hashimoto, T. Sugahara and K. Ohgaki, "Thermodynamic Stability of Hydrogen+Tetra-n-Butyl Phosphonium Bromide Mixed Semi-Clathrate Hydrate," *Chem. Eng. Sci.*, vol. 68, p. 660–662, 2012.

[66] J. Du, L. Wang, D. Liang and D. Li, "Phase Equilibria and Dissociation Enthalpies of Hydrogen Semi-Clathrate Hydrate with Tetrabutyl Ammonium Nitrate," *J. Chem. Eng. Data*, vol. 57, p. 603–609, 2012.

[67] S. Hashimoto, T. Tsuda, K. Ogata, T. Sugahara, Y. Inoue and K. Ohgaki, "Thermodynamic Properties of Hydrogen + Tetra-n-Butyl Ammonium Bromide Semi-Clathrate Hydrate," *Journal of Thermodynamics*, p. 5, 2010.

[68] S. Hashimoto, S. Murayama, T. Takeshi, H. Sato and K. Ohgaki, "Thermodynamic and Raman spectroscopic studies on H2 + tetrahydrofuran + water and H2+ tetra-n-butyl ammonium bromide + water mixtures containing gas hydrates," *Chem. Eng. Sci.*, vol. 61, pp. 7884-7888, 2006.

[69] A. A. Karimi, O. Dolotko and D. Dalmazzone, "Hydrate phase equilibria data and hydrogen storage capacity measurement of the system H2 + tetrabutylammonium hydroxide + H2O," *Fluid Phase Equilibria*, vol. 361, pp. 75-180, 2014.

[70] J. Deschamps and D. Dalmazzone, "Hydrogen Storage in Semiclathrate Hydrates of Tetrabutyl Ammonium Chloride and Tetrabutyl Phosphonium Bromide," *J. Chem. Eng. Data,* vol. 55, p. 3395–3399, 2010.

[71] L. J. Florusse, C. J. Peters, j. Schoonman, K. C. Hester, C. A. Koh, S. F. Dec, K. N. Marsh and E. D. Sloan, "Stable Low-Pressure Hydrogen Clusters Stored in a Binary Clathrate Hydrate," *Science,* vol. 306, pp. 469-471, 2004.

[72] M. Arjmandi, A. Chapoy and B. Tohidi, "Equilibrium Data of Hydrogen, Methane, Nitrogen, Carbon Dioxide, and Natural Gas in Semi-Clathrate Hydrates of Tetrabutyl Ammonium Bromide," *J. Chem. Eng. Data,* vol. 52, pp. 2153-2158, 2007.

[73] S. Lee, Y. Lee, S. Park and Y. Seo, "Phase Equilibria of Semiclathrate Hydrate for Nitrogen in the Presence of Tetra-n-butylammonium Bromide and Fluoride," *J. Chem. Eng. Data,* p. 5883–5886, 2010.

[74] A. Eslamimanesh, Thermodynamic Studies on Semiclathrates Hydrates of TBAB+ Gases Containing Carbon Dioxide,Ph.D. Dissertation, Paris: MINES ParisTech, 2012.

[75] J. H. van der Waals and J. C. Platteeuw, "Clathrate Solutions," *Advances in Chemical Physics,* pp. 1-57, 1959.

[76] W. R. Parrish and J. M. Prausnitz, "Dissociation Pressures of Gas Hydrates Formed by Gas Mixtures," *Ind. Eng. Chem. Process Des> Develop.,* vol. 11, no. 1, pp. 26-35, 1972.

[77] P. L. Chueh and J. M. Prausnitz, "Vapor-liquid Equilibria at High Pressures. Vapor-phase Fugacity Coefficients in Nonpolar and Quantum-gas Mixtures," *Ind. Eng Chem. Fundam,* vol. 6, pp. 492-498, 1967.

[78] G. D. Holder, G. Corbin and K. D. Papadopoulos, "Thermodynamic and Molecular Properties of Gas Hydrates from Mixtures Containing Methane, Argon, and Kripton," *Ind. Eng. Chem. Fundam.*, vol. 19, pp. 282-286, 1980.

[79] A. H. Mohammadi, V. Belandria and D. Richon, "Use of an Artifical Neural Network Algorithm to Predict Hydrate Dissociation Conditions for Hydrogen+Water and Hydrogen+tetra-n-butyl ammonium Bromide+Water Systems," *Chem. Eng. Sci.*, vol. 65, pp. 4302-4305, 2010.

[80] A. Joshi, P. Mekala and J. M. Sangwai, "Modeling Phase Equilibria of Semiclathrates hydrates of CH4,CO2 and N2 in aqueous Solutions of Tetra-n-butyl ammonium Bromide," *Journal of Natural Gas Chemistry*, vol. 21, pp. 459-465, 2012.

[81] G. J. Chen and T. M. Guo, "Thermodynamic Modeling of Hydrate Formation Based on New Concepts," *Fluid Phase Equilibria*, vol. 122, pp. 43-65, 1996.

[82] G. J. Chen and T. M. Guo, "A New Approach to Gas Hydrate Modeling," *Chem. Eng. J.*, vol. 71, pp. 145-151, 1998.

[83] Z. Liao, X. Guo, Y. Zhao, Y. Wang, Q. Sun, A. Liu, C. Sun and G. Chen, "Experimental and Modeling Study on Phase Equilibria of Semiclathrates Hydrates of Tetra-n-butyl Ammonium Bromide+CH4,C02,N2, or Gas Mixtures," *Ind. Eng. Chem. Res.*, vol. 52, pp. 18440-18446, 2013.

[84] N. C. Patel and A. S. Teja, "A New Cubic Equation of State for Fluids and Fluid Mixtures," *Chem. Eng. Sci.*, vol. 37, pp. 463-473, 1982.

[85] S. Babaee, H. Hashemi, A. H. Mohammadi, P. Naidoo and D. Ramjugernath, "Experimental Measurement and Thermodynamic Modeling of Hydrate Dissociation Conditions for the Argon+TBAB+Water System," *J. Chem. Eng. Data,* vol. 59, pp. 3900-3906, 2014.

[86] A. Eslamimanesh, A. H. Mohammadi and D. Richon, "Thermodynamic Modeling of Phase Equilibria of Semiclathrate Hydrates of CO2, CH4, or N2+Tetra-n-butyl Ammonium Brimide Aqueous Solution," *Chemical Engineering Science,* vol. 81, pp. 319-328, 2012.

[87] D. Y. Peng and D. B. Robinson, "A New Two-constant Equation of State," *Ind. Eng. Chem. Fundam,* vol. 15, pp. 59-64, 1976.

[88] P. M. Mathias and T. W. Copeman, "Extension of the Peng-Robinson Equation of State to Complex Mixtures: an Evaluation of the Various Forms of the Local Composition Concept," *Fluid Phase Equilibria,* vol. 13, pp. 91-108, 1983.

[89] L. L. Shi and D. Q. Liang, "Thermodynamic Model of Phase Equilibria of Tetrabutyl Ammonium Halide (fluoride,chloride, or bromide) Plus Methane or Carbon Dioxide Semiclathrates Hydrates," *Fluid Phase Equilibria,* vol. 386, pp. 149-154, 2015.

[90] P. Paricaud, "Modeling the Dissociation Conditions of Salt Hydrates and Gas Semiclathrate Hydrates: Application to Lithium Bromide, Hydrogen Iodine, and Tetra-n-butylammonium Bromide + Carbon Dioxide systems," *J.Phys. Chem,* vol. 115, pp. 288-299, 2011.

[91] A. Fukumoto, P. Paricaud, D. Dalmazzone, W. Bouchafaa and T. T. Ho, "Modeling Dissociation Conditions of Carbon Dioxide+TBAB,TBAC,TBAF, and TBPB Semiclathrates Hydrates," *J. Chem. Eng. Data*, vol. 59, p. 3193, 2014.

[92] A. Galindo, A. Gil-Villegas, G. Jackson, G. Burgess and M. Radosz, "SAFT-VRE: Phase Behavior of Electrolyte Solutions with the Statistical Associating Fluid Theory for Potentials of Variable Range," *J. Phys. Chem.*, vol. 103, pp. 10272-10281, 1999.

[93] M. Kwaterski and J. Herri, "Thermodynamic Modeling of Gas Semi-Clathrate Hydrates Using the Electrolyte NRTL Model," in *7th International Conference on Gas Hydrates*, Edimbourg, 2011.

[94] J. Verrett, J. S. Renault-Crispo and P. Servio, "Phase equilibria, solubility and modeling study of CO2/CH4 + tetra-n butylammonium bromide aqueous semi-clathrate systems," *Fluid Phase Equilibria*, vol. 388, pp. 160-168, 2015.

[95] J. Gmehling, B. Kolbe, M. Kleiber and J. Rarey, Chemical Thermodynamics for Process Simulation, Boschtr: Wiley-VCH, 2012.

[96] W. Yan, M. Topphoff, C. Rose and J. Gmehling, "Prediction of Vapour-Liquid Equilibria in Mixed-solvent Eelctrolyte Systems Using the Group Contribution Concept," *Fluid Phase Equilibria*, vol. 162, pp. 97-113, 1999.

[97] M. A. Clarke and P. R. Bishnoi, "Development of an Implicit Least Squares Optimisation Scheme for the Determination of Kihara Potential Parameters Using Gas Hydrate equilibrium Data," *Fluid Phase Equilibria*, vol. 211, pp. 51-60, 2003.

[98] M. Kwaterski and J. M. Herri, "Modelling of gas clathrate hydrate equilibria using the electrolyte non-random two-liquid (eNRTL) model," *Fluid Phase Equilibria*, vol. 371, pp. 22-40, 2014.

[99] T. Kihara, "On Isihara-Hayashida's Theory of the Second Virial Coefficient for Rigid Convex Molecules," *J. Phys. Soc. Japan*, vol. 8, pp. 686-687, 1953.

[100] T. Kihara, "Virial Coefficients and Models of Molecules in Gases," *Rev. Mod Phys.*, vol. 25, pp. 831-840, 1953.

[101] V. McKoy and O. Sinanoglu, "Theory of Dissociation Pressures of Some Gas Hydrates," *J. Chem. Phys.*, vol. 38, pp. 2485-2490, 1963.

[102] J. A. Nelder and R. A. Mead, "A Simplex Method for Function Minimization," *Computer Journal*, vol. 7, pp. 308-313, 1965.

[103] A. Constantinides and N. Mostoufi, Numerical Methods for Chemical Engineers with Matlab Applications, New Jersey: Prenticel Hall PTR, 1999.

[104] H. H. Rachford and J. D. Rice, "Procedure for Use of Electronic Digital Computers in Calculating Flash Vaporization Hydrocarbon Equilibrium," *J. Pet. Technol.*, vol. 4, pp. 10-14, 1952.

[105] T. Holderbaum and J. Gmehling, "PSRK: A Group Contribution Equation of State Based on UNIFAC," *Fluid Phase Equilibria*, vol. 70, pp. 251-265, 1991.

[106] G. Soave, "Equilibrium Constants from a Modified Redlich-Kwong Equation of State," *Chem. Eng. Sci.*, vol. 27, pp. 1197-1203, 1972.

[107] P. M. Mathias and T. W. Copeman, "Extension of the Peng-Robinson Equation of State to Complex Mixtures," *Fluid Phase Equilibria*, vol. 13, pp. 91-108, 1983.

[108] M. L. Michelsen, "A Method for Incorporating Excess Gibbs Energy Models in Equations of State," *Fluid Phase Equilibria*, vol. 60, pp. 47-58, 1990.

[109] A. Fredenslund, R. L. Jones and J. M. Prausnitz, "Group-Contribution Estimation of Activity Coefficients in Nonideal Liquid Mixtures," *AIChE. J.*, vol. 21, no. 6, pp. 1086-1099, 1975.

[110] D. S. Abrams and J. M. Prausnitz, "Statistical Thermodynamics of Liquid Mixtures: A New Expression for the Excess Gibbs Energy of Partly or Completely Miscible Systems," *AIChE J.*, vol. 21, pp. 116-128, 1975.

[111] J. Li, M. Topphoff, K. Fischer and J. Gmehling, "Prediction of Gas Solubilities in Aqueous Electrolyte Systems Using the Predictive-Soave-Redlich-Kwong Model," *Ind. Eng. Chem. Res.*, vol. 40, pp. 3703-3710, 2001.

[112] J. Kiepe, S. Horstmann, K. Fischer and J. Gmehling, "Experimental Determination and Prediction of Gas Solubility Data for Methane+Water Solutions Containing DIfferent Monovalent Electrolytes," *Ind. Eng. Chem. Res.*, vol. 42, pp. 5392-5398, 2003.

[113] J. Kiepe, S. Horstmann, K. Fischer and J. Gmehling, "Application of the PSRK Model for Systems Containing Strong Electrolytes," *Ind. Eng. Chem. Res.*, vol. 43, pp. 6607-6615, 2004.

[114] J. R. Elliot and C. T. Lira, Introductory Chemical Engineering Themodynamics, New Jersey: Prentice Hall PTR, 1999.

APPENDIX A: ISOTHERMAL ISOBARIC FLASH COMPUTATION

Flash calculations can be defined as a process of calculating the mole fractions, x_i and y_i, in the liquid phase and vapour phase respectively at the prevailing pressure and temperature when given the overall composition of the mixture, z_i , as shown in Figure A.1

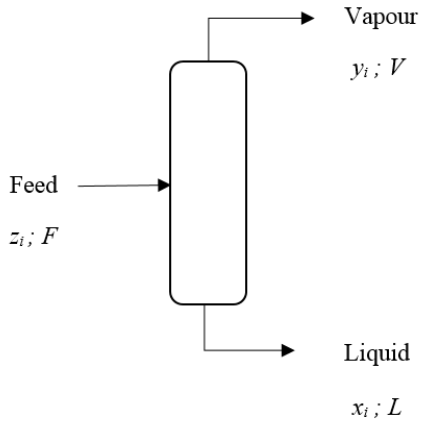

Figure A.1: Scheme of vapor-liquid isothermal flash

The below following equations constrains the vapour and liquid phase mole, where the summation of molar fraction in both vapour and liquid phase should be equal to unity:

$$\sum_{i=1}^{c} y_i = \sum_{i=1}^{c} x_i = 1 \qquad \textbf{(A.1)}$$

The *K*-value or the equilibrium ratio of component *i* is given by the following expression below:

$$K_i = \frac{y_i}{x_i} = \frac{\varphi_i^L}{\varphi_i^V} \rightarrow y_i = K_i x_i \qquad \textbf{(A.2)}$$

The partial fugacity coefficients are represented as φ_i^L, φ_i^V which are calculated by using the PSRK EoS in the present work and are presented in Appendix B. On the basis of one mole; the summation of the vapour and liquid mole fractions is the unity (F = 1); i.e. L+V = 1. For *i* component the material balance is given by the following expression below:

$$z_i = y_i V + x_i L \qquad \textbf{(A.3)}$$

$$z_i = y_i V + x_i(1 - V) \quad \textbf{(A.4)}$$

When substitution yi from Equation (A.2) in Equation (A.4) we get the following expression below:

$$z_i = y_i V x_i K_i + (1 - V) x_i \quad \textbf{(A.5)}$$

When equation (A.5) is solved for x_i

$$x_i = \frac{z_i}{1 + V(K_i - 1)} \quad \textbf{(A.6)}$$

Solving Equation (A.4) for y_i yields:

$$y_i = K_i x_i = \frac{z_i K_i}{1 + V(K_i - 1)} \quad \textbf{(A.7)}$$

When substituting Equation (A.6) and Equation (A.7) into Equation (A.1) we get the following expression below:

$$\sum_{i=1}^{c} y_i = \sum_{i=1}^{c} x_i = \sum_{i=1}^{c} (y_i - x_i) = \sum_{i=1}^{c} \frac{z_i(K_i - 1)}{1 + V(K_i - 1)} = 0 \quad \textbf{(A.8)}$$

The above equation (A.8) is known as the Rachford-Rice equation [104] in which *V* is the only unknown term, the equation (A.8) can be rewritten as an implicit function of *V*:

$$f(V) = \sum_{i=1}^{c} \frac{z_i(K_i - 1)}{1 + V(K_i - 1)} = 0 \quad \textbf{(A.10)}$$

The algorithm to solve Equation (A.10) is presented in The Figure A.2, provides the algorithm to solve the Equation (A.10).

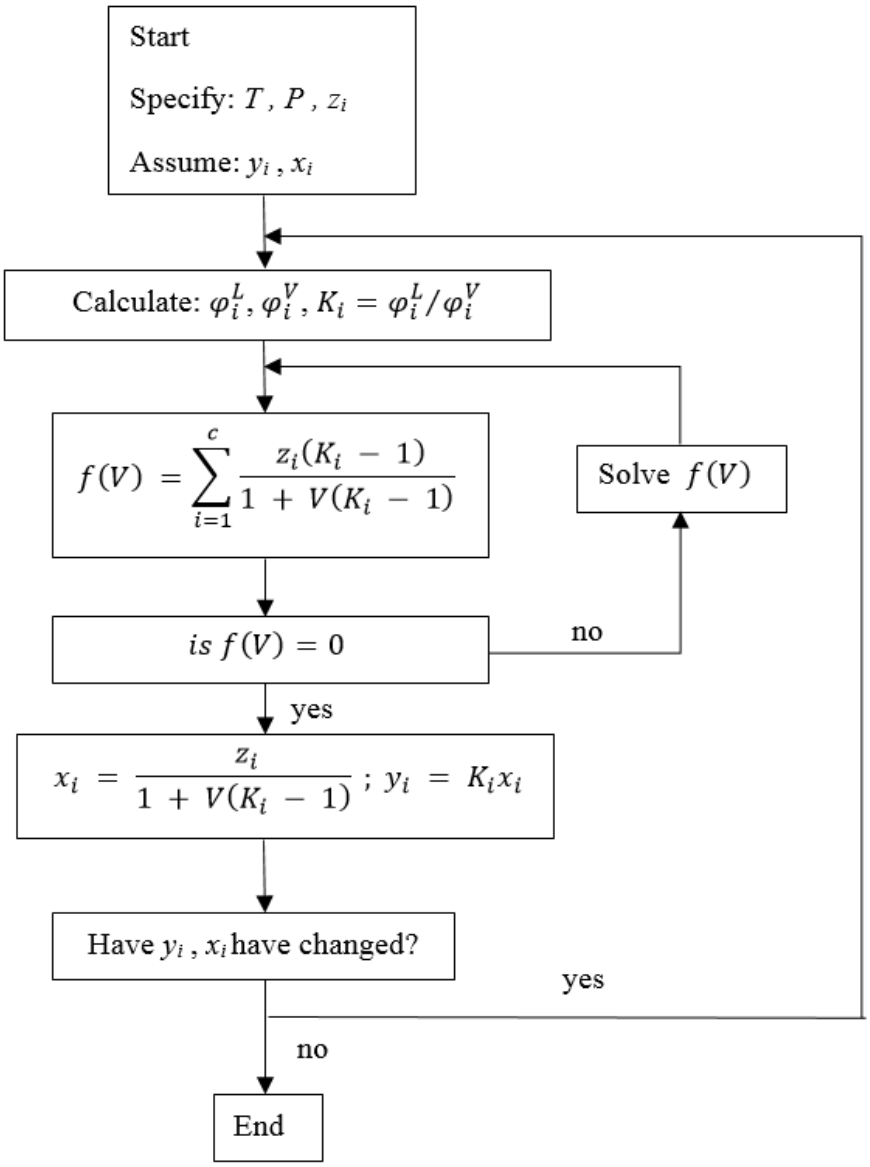

Figure A.2: Algorithm for solving the isothermal flash (Reproduced from Elliot and Lira (*114*)

APPENDIX B: ANALYTICAL SOLUTION TO CUBIC EQUATIONS

A cubic equation of state can be solved by two different approach either by trial and error or by analytically. In our present work the roots of the equation of state are calculated by analytical approach. The compressibility factor, z in terms of any cubic equation of the state is given by the expression [95]:

$$z^3 + Uz^2 + Sz + T = 0 \tag{C.1}$$

With the following abbreviations:

$$P = \frac{3S - U^2}{2} \tag{C.2}$$

$$Q = \frac{2U^3}{27} - \frac{US}{3} + T \tag{C.3}$$

The discriminant can be determined to be

$$D = \left(\frac{P}{3}\right)^3 + \left(\frac{Q}{2}\right)^2 \tag{C.4}$$

When *D*>0, the equation has only one real root:

$$z = \left(\sqrt{D} - \frac{Q}{2}\right)^{1/3} - \frac{P}{\left(3\left(\sqrt{D} - \frac{Q}{2}\right)^{\frac{1}{3}}\right)} - \frac{U}{3} \tag{C.5}$$

When *D*<0, there are three real roots.

$$\Theta = \sqrt{-\frac{P^3}{27}}\ and\ \Phi = \arccos\left(\frac{-Q}{2\Theta}\right) \tag{C.6}$$

The roots of the equation are given by the following expressions below:

$$z_1 = 2\Theta^{1/3} cos\left(\frac{\Phi}{3}\right) - \frac{U}{3} \tag{C.7}$$

$$z_2 = 2\Theta^{1/3} cos\left(\frac{\Phi}{3} + \frac{2\pi}{3}\right) - \frac{U}{3} \tag{C.8}$$

$$z_3 = 2\Theta^{1/3} cos\left(\frac{\Phi}{3} + \frac{4\pi}{3}\right) - \frac{U}{3} \qquad \textbf{(C.9)}$$

The largest and the smallest of the three roots correspond to the vapour and to the liquid, respectively. The middle root does not have any physical meaning.

APPENDIX C: ERROR CALCULATION IN THE PARAMETER ESTIMATION

The standard error of the parameters is calculated once all the parameters are estimated. The standard error is calculated by the square root of the corresponding diagonal element of the inverse of the matrix ***A**** multiplied by the variance [97].

$$\hat{\sigma}_{k_i} = \hat{\sigma}_{\varepsilon}\sqrt{\{[A^*]\}_{ii}} \quad \textbf{(D.1)}$$

Where:

$$\hat{\sigma}_{\varepsilon} = \frac{F\left(a_{n,m}, b_{n,m}\right)}{d.f.} \quad \textbf{(D.2)}$$

$$A = \sum_{i=1}^{NP}\left[\frac{\partial \boldsymbol{e}^T}{\partial \boldsymbol{k}}\right]\cdot\left[\frac{\partial \boldsymbol{e}^T}{\partial \boldsymbol{k}}\right]^T \quad \textbf{(D.3)}$$

$$e_i = x_{gas}^{calc} - x_{gas}^{exp} \quad \textbf{(D.4)}$$

Vector of estimated parameters is represented as ***k***,.The standard error of parameter is represented as $\hat{\sigma}_{k_i}$. The ki *d.f*, is the degrees of freedom, which are given by the number of experimental points minus the number of parameters.

APPENDIX D: PRIVATE COMMUNICATION WITH KWATERSKI:

Dear Matthew
Please find the answer of Matthias Kwaterski
Best regards,

Well, I have checked the results of the co-worker of Mr Clarke and they are basically correct except from a minor error: the gamma values as well as the absolute values of the results for delta_diss_G_0 are correct, however, they have to be multiplied by -1. In other words, the numerical values of delta_diss_G_0 have to be positive. In the formula for delta_diss_G_0 of the 38-semi-clathrate as presented in his MS Word document, he erroneously wrote 285,15 K. Of course, this temperature value should be replaced by 283,5 K, but I've checked the results provided in his table and they are correctly calculated. Thus, when using the isothermal parameter values for the eNRTL parameters at 298,15 K, I ended up at the numerical results 24438,6 J mol-1 and 25378,5 J mol-1 for delta_diss_G_0 of the 26 and the 38 semi-clathrate hydrate, respectively. With except from the sign, these values do match with the values I have calculated. Therefore, also the calculated gamma values (table two in the MS Word document) as well as the values presented in table 1 do match with my results. That further means that the values cited in the poster shown in China were unfortunately not presented correctly.

Le 19/01/2015 18:18, Matthew Clarke a écrit :
Dear Jean-Michel,
How are you? I have a student who is currently working on computing equilibrium in semi-clathrates, using your approach, and he is having difficulty reproducing your values for the Gibbs Free Energy Change of Dissociation. I have asked him to type up a detailed sample calculation to show the numbers that he is using to compute the Gibbs Free Energy Change and I have attached this document. In this document he not only shows his calculation of ΔG but he also shows that his eNRTL model reproduces the results of Chen. Can you kindly take a moment to compare his numbers with yours? I've been working with my student for over a month and I'm not able to see any glaringly obvious mistakes in his numbers. Perhaps we have misinterpreted something that was written?
Thank you for your time Jean-Michel

Matthew Clarke